CHARLES UNIVERSITY IN PRAGUE

Faculty of Pharmacy in Hradec Králové

Department of Pharmacology and Toxicology

ANTI-INFLAMMATORY EFFECTS OF URSODEOXYCHOLYL LYSOPHOSPHATIDYLETHANOLAMIDE ON THP-1 HUMAN MACROPHAGES VIA TOLL-LIKE RECEPTOR 4

Diploma thesis

Supervisor: Prof. PharmDr. Petr Pávek PhD.

Hradec Králové, 2016

Alžbeta Horvátová

Statutory Declaration

"I declare that the enclosed diploma thesis represents my own research work without undue help from second person. I have clearly documented all of literal sources and material used. The diploma thesis was not used in the same or in a similar version to achieve an academic grading or is being published elsewhere."

Hradec Králové, 30.04.2016 Alžbeta Horvátová

Acknowledgement

I would like to express my sincere gratitude to Dr. Walee Chamulitrat for giving me a great opportunity to become a member of her research group and preparing this project for me, for being a perfect advisor and leader at the same time. Then, I would like to say a big thank you to Tanyarath Utaipan for showing me all I needed to perform experiments in this study, for her consultations and inspiration. And also, I would like to thank to my Czech supervisor, Prof. Petr Pávek for professional leadership of my diploma thesis. Thank you!

Abstract

Charles University in Prague

Faculty of Pharmacy in Hradec Králové

Department of Pharmacology & Toxicology

Student: Alžbeta Horvátová

Supervisor: prof. PharmDr. Petr Pávek PhD.

Title of diploma thesis:

Anti-inflammatory effects of ursodeoxycholyl lysophosphatidylethanolamide on THP-1 human macrophages via Toll-like receptor 4

Nonalcoholic steatohepatitis (NASH) became the most common liver disease in developed countries. It is well-known that the level of protectant phosphatidylcholine (PC) is decreased in NASH. The bile acid-phospholipid conjugate ursodeoxycholyl lysophosphatidylethanolamide (UDCA-LPE) was designed in order to specifically deliver PC to hepatocytes. However, previous studies have proved that UDCA-LPE possesses its proper hepatoprotectant capacity and exhibits anti-apoptotic, anti-inflammatory, anti-fibrotic properties and also improved steatosis and hyperlipidaemia in various models *in vivo*. These effects may be mediated secondary through modulation of immune system. Therefore, in order to dissect if UDCA-LPE directly influences immune cells *in vitro*, release of pro-inflammatory cytokines TNFα, IL-6 and IL-1β in LPS-induced THP-1-derived human macrophages was measured by ELISA. Moreover, effects of UDCA-LPE on MAPK signalling pathways and nuclear translocation of NFκB were determined by Western blot analysis and immunofluorescence. For deeper investigation, lipid rafts were isolated using Optiprep gradient and recruitment of adaptor proteins TRAF6 and MyD88 into the lipid rafts was assessed by Western blot analysis. UDCA-LPE was able to significantly inhibit release of all measured pro-inflammatory cytokines, nuclear translocation of NFκB and activation of MAPK members JNK1/2 and p38. We therefore may anticipate that UDCA-LPE can exhibit its hepatoprotective properties via modulation of immune system in LPS-induced inflammatory response. Due to its versatility, UDCA-LPE has a potential to become a novel therapeutic approach for treatment of NASH.

Abstrakt

Univerzita Karlova v Praze

Farmaceutická fakulta v Hradci Králové

Katedra farmakologie a toxikologie

Studentka: Alžbeta Horvátová

Školitel: prof. PharmDr. Petr Pávek PhD.

Název diplomové práce:

Protizánětlivý účinek UDCA-LPE na lidské makrofágové buněčné linii THP-1 prostřednictvím Toll-like receptoru 4

Nealkoholická steatohepatitida (NASH) se stala jedním z nejčastějších onemocnění jater v rozvinutých zemích. Během NAFLD je hladina ochranného fosfatidylcholinu (PC, z angl. phosphatisylcholine) snížena. Fosfolipidový konjugát žlučové kyseliny ursodeoxycholyl lysofosfatidylethanolamin (UDCA-LPE) byl navržen, aby specificky zabezpečil dodávku PC do hepatocytů. Nicméně, předchozí studie prokázaly, že UDCA-LPE má svůj vlastní hepatoprotektivní účinek a vykazuje anti-apoptické, protizánětlivé, anti-fibrotické vlastnosti a rovněž zlepšuje steatózu a hyperlipidemii na různých modelech *in vivo*. Tyto účinky mohou být zprostředkovány sekundárně prostřednictvím modulace imunitního systému. Z tohoto důvodu, s cílem zjistit jestli má UDCA-LPE přímý vliv na buňky imunitního systému *in vitro*, jsem změřila pomocí ELISA uvolňování prozánětlivých cytokinů TNFα, IL-6 a IL-1β v LPS-indukovaných THP-1-derivovaných lidských makrofázích. Kromě toho účinek UDCA-LPE na MAPK signální dráhy a nukleární translokaci NFκB byl stanoven Western blot analýzou a imunofluorescencí. Pro hlubší šetření, lipidové rafty byly izolovány s použitím Optiprep gradientu a nábor adaptorových proteinů TRAF6 a MyD88 do lipidové rafty byl zhodnocen Western blot analýzou. UDCA-LPE byl schopen významně inhibovat uvolňování všech změřených pro-zánětlivých cytokinů, nukleární translokaci NFκB a aktivaci MAPK členů JNK1/2 a p38. Proto můžeme předpokládat, že UDCA-LPE může vykazovat své hepatoprotektivní vlastnosti prostřednictvím modulace imunitního systému v LPS-indukované zánětlivé odpovědi. Vzhledem ke své všestrannosti UDCA-LPE má potenciál stát se novým terapeutickým přístupem pro léčbu NASH.

1 TABLE OF CONTENT

2 LIST OF ABBREVIATIONS

AIM2 – absence in melanoma 2

AP-1 – activator protein 1

APS – ammonium persulfate

ATF-2 – activating transcription factor 2

BA – bile acid

BPB – bromphenol blue

BSA – bovine serum albumin

CA – cholic acid

CD14 – cluster of differentiation 14

CDCA – chenodeoxycholic acid

CLR – C-type lectin receptor

COX-2 – cyclooxygenase 2

DAMP – damage-associated molecular pattern

DAPI - 4,6'-diamidino-2-phenylindole

DCA – deoxycholic acid

DNA – deoxyribonucleic acid

DRM – detergent resistant membrane

ECL – electrochemiluninescence

ELISA – enzyme-linked immunosorbent assay

ER – endoplasmic reticulum

ERK – extracellular signal-regulated kinase

FBS – foetal bovine serum

FXR – farnesoid X receptor

FTIC – fluorescin isothicyanate

GAPDH – glyceraldehyde 3-phosphate dehydrogenase

GPI – glycosylphosphatidylinositol

GTP - guanosinetriphosphate

HMGB – high mobility group box

HPLC – high-performance liquid chromatography

HRP – horseradish peroxidase

HSP – high shock protein

IFN – interferon

IFR-3 – interferon regulatory factor 3

IKK – IκB kinase

IL – interleukin

IL-1R – interleukin-1 receptor

iNOS – inducible nitric oxide synthetase

IRAK – IL-1R associated kinase

IRF-3 – interferon regulatory factor 3

JNK – c-Jun N-terminal kinase

LBP – lipopolysaccharide binding protein

LCA – litocholic acid

LPE - lysophosphatidyethanolamine

LPS - lipopolysacharide

LRR – leucine rich region

LXR – liver X receptor

MAPK – mitogen activated protein kinase

MAPKK, MKK – MAPK kinase

MAPKK – MAPKK kinase

MyD88 – myeloid differentiation factor 88

NADPH – nicotinamide adenine dinucleotide phosphate

NAFLD – non-alcoholic fatty liver disease

NASH – non-alcoholic steatohepatitis

NEMO – NFκB essential modulator

NLR -Nod-like receptor

NFκB – nuclear factor kappa B

PAMP – pathogen-associated molecular pattern

PBC – primary biliary cirrhosis

PBS – phosphate-buffered saline

PC – phosphatidylcholine

PE – phosphatidylethanolamine

PEMT – phosphatidylethanolamine methyltransferase

PGE2 – prostaglandin E2

PMA – phorbol 12-myristate 13-acetate

PMSF – phenylmethylsulfonyl fluoride

PRR – pattern recognition receptor

PSC – primary sclerosing cholangitis

PUFA – polyunsaturated fatty acids

PVDF – polyvinylidene fluoride

RIG-I – retinoid-acid-inducible gene I

RLR – RIG-I like receptor

RNA – ribonucleic acid

RPMI – Roswell Park Memorial Institute

ROS – reactive oxygene species

SDS – sodium dodecyl sulfate

SDS-PAGE – SDS-polyacrylamide gel electrophoresis

TAK – transforming growth factor β-activated kinase

TBS – Tris-buffered saline

TEMED - tetramethylethylenediamine

TGR5 – G-coupled protein receptor specific for bile acids

TIR – Toll/interleukin-1 receptor

TLR – Toll-like receptor

TMB - tetramethylbenzidine

TNF – tumor necrotizing factor

TRAF6 – TNF receptor associated factor 6

TRIF – Toll/interleukin-1R domain containing adaptor incuding interferon β

TRITC – tetramethylrhodamine isocyanate

UDCA – ursodeoxycholic acid

UDCA-LPE – ursodeoxycholyl lysophosphatidylethanolamide

USA – United States of America

3 INTRODUCTION

Nonalcoholic steatohepatitis (NASH) became the most common liver disease in developed countries (2-6% of western population is affected). Fat accumulation in the liver with subsequent inflammation that may result into liver fibrosis are the main characteristic of this pathology. It is well-known that the level of phosphatidylcholine (PC) which helps to maintain membrane integrity is decreased in NASH.

The bile acid-phospholipid conjugate ursodeoxycholyl lysophosphatidyl-ethanolamide (UDCA-LPE) was synthetized in order to specifically deliver PC to liver. However, previous studies have proved that UDCA-LPE does not hydrolyse in hepatocytes as expected but surprisingly it possesses its proper hepatoprotectant capacity and exhibits anti-apoptotic, anti-inflammatory, anti-fibrotic properties and also improved steatosis and hyperlipidaemia in various models *in vivo*.

These effects may be mediated secondary through modulation of immune system, especially when UDCA-LPE exhibits strong anti-inflammatory properties. For this reason, the ability of this bile acid-phospholid conjugate to affect inflammatory signalling pathway in macrophages will be assessed in this research work.

4 THEORETICAL PART

4.1 Inflammation and innate immunity

Innate immune system functions as a primary defense system to recognize, rapidly react and restore altered physiological environment caused by exogenous and endogenous harmful stimuli. These factors initiate intracellular inflammatory signaling pathways in macrophages resulting in production and release of potent inflammatory mediators including cytokines like interleukin 1β (IL-1β), tumor necrotizing factor α (TNFα) or interleukin 6 (IL-6); chemokines and interferons and also toxic molecules such as nitric oxide or free radicals which in turn mobilize further immune cells and lymphocytes to ensure an appropriate inflammatory reaction to a specific insult. Inflammation is highly regulated and there is no doubt that it plays a key role in host protection and maintenance of physiological homeostasis. However, disruption of its control, deficiency as well as excess of the inflammatory response, has deleterious effects that perturb regular hemodynamic and metabolic balances leading to a variety of disease including chronic inflammation, autoimmunity and neurodegenerative disorders or immunodeficiency on the other side. The fact that a wide variety of physical, chemical and biological agents are able to trigger different signaling pathways underlies the importance of their regulation (Kaminska 2005, Lin and Yeh 2005, Kim, Ahn et al. 2011).

To monitor the local environment for signs of danger, specialized immune cells such as macrophages and dendritic cells possess on their cellular membranes and even in the cytosolic compartments families of highly conserved pattern recognition receptors (PRRs). The innate immunity encompasses Toll-like receptors (TLRs), Nod-like receptors (NLRs), surface expressed C-type lectin receptors (CLRs), cytosolic retinoic-acid-inducible gene I (RIG-I)-like receptors (RLRs), and several cytosolic DNA receptors including absence in melanoma 2 (AIM2) (Broz and Monack 2013). PRRs are able to detect invading microbial pathogens by recognizing conserved pathogen-associated molecular patterns (PAMPs) but they also can be activated by multiple endogenous damage-associated molecular patterns (DAMPs) host-derived from tissue damage or stress and induce sterile inflammation. According to up-to-date

evidence, PRRs also provide maintenance of disrupted immunity and metabolic homeostasis. (Huang, Rutkowsky et al. 2012).

4.1.1 Characterization of Toll-like receptors

Among all PRRs, family of TLRs is the most notorious and studied one. TLRs are transmembrane receptors composed of three structural regions (Figure 1). Its external part providing ligand recognition is characterized by amino N-terminal domain consisting of leucin rich region (LRRs) giving typical bended horseshoe-like shape, then a single membrane-spanning region and intracellular carboxyl C-terminal Toll/interleukin-1 receptor (TIR) signaling domain. This highly conserved cytoplasmic domain is characteristic of the Interleukin-1 receptor/Toll-like receptor superfamily (Ruysschaert and Lonez 2015). Binding ligands usually promote dimerization of TLRs followed by conformational changes in TIR domains favouring the activation of downstream signalling succession, extracellular TLRs have been shown to exist as preformed homodimers (De Nardo 2015), whilst TLR2 tend to heterodimerize with TLR1 or TLR6 when activated, TLR4 is known to form more likely homodimers (Reuven, Fink et al. 2014).

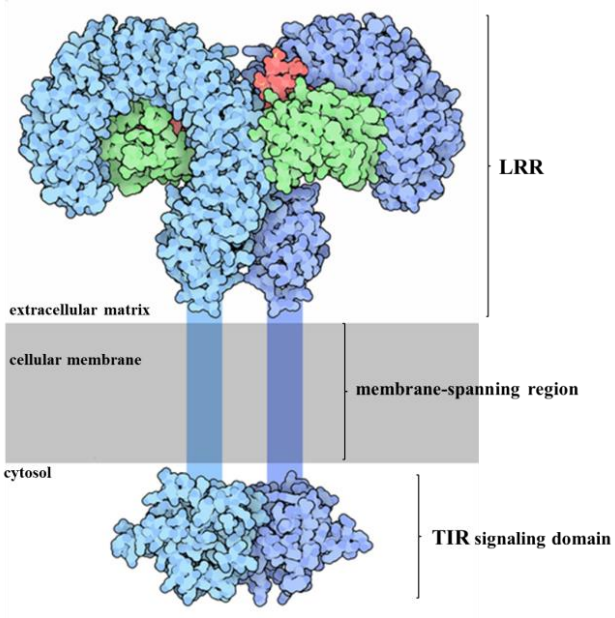

Figure 1: Structure of TLR4, homodimer of the TLR4 is presented in blue, accessory protein MD-2 in green, and LPS in red. Modified according to: http://pdb101.rcsb.org/motm/143.

Ten different TLRs have been identified in human immune cells and can be divided in two major categories in dependence of their cellular localization. On the cell surface, TLR1, TLR2, TLR4, TLR5, TLR6 and TLR10 are expressed whereas TLR3, TLR7, TLR8, and TLR9 reside in intracellular vesicles. Different TLRs are able to perceive different ligands. Extracellular ones evolved to sense bacterial and fungal PAMPs while intracellular TLRs are specialized more in viral nucleic acid detection. Concise summary of TLR ligands is in the Table 1 below (Brubaker, Bonham et al. 2015, Jimenez-Dalmaroni, Gerswhin et al. 2016). Moreover, pathogenic species usually can be perceived not only by different TLRs but also by various PRRs. This complexity provides multiplex surveillance over harmful signals (Blasius and Beutler 2010).

TLR	**Microbial ligand (PAMPs)**	**Endogenous ligand (DAMPs)**
extracellular		
➢ TLR4	Lipopolysaccharide (Gram-negative bacteria), taxol,	Saturated fatty acid, hyaluronic acid, fibrinogen, fibronectin, heat shock protein (HSP) 60, HSP70, biglycan, oxided LDL
➢ TLR2 (in association with TLR 1 or TLR6)	Lipoteichoic acid (Gram positive bacteria), lipomannan (Mycobacterium) di-acylated and tri-acylated bacterial lipopeptides, herpes simplex virus, human cytomegalovirus	HSP60, HSP70, biglycan, HMGB-1
➢ TLR5	Flagelin	unknown
intracellular		
➢ TLR3	Double stranded viral RNA	mRNA from necrotic cells
➢ TLR7	Single stranded RNA	Single stranded RNA
➢ TLR8	Single stranded RNA	Single stranded RNA
➢ TLR9	CpG motif RNA	Self-DNA

Table 1: Summary of TLR ligand, modified according to (Brubaker, Bonham et al. 2015, Jimenez-Dalmaroni, Gerswhin et al. 2016).

4.1.2 Lipopolysacharide signaling via Toll-like receptor

Lipopolysaccharide (LPS) is the principal component of the outer membrane of Gram-negative bacteria sensed by monocyte and macrophage cell lineage and is broadly

used as initiator of inflammatory signaling pathway in *in vitro* and *in vivo* studies. LPS acts through TLR4, stimulates mitogen-activated protein kinase (MAPK) cascades as well as the pathway leading to activation of nuclear factor κB (NFκB). Human immune network has evolved sensitive system to detect even low level LPS in the bloodstream. First, LPS is linked to LPS binding protein (LBP). Normal concentration of LBP in human plasma is 4.1±1.65 μg/ml (Opal, Scannon et al. 1999) but its level increases rapidly during inflammatory response. LBP-opsonized particles are delivered to cell surface receptor CD14, a myeloid marker protein, whose presence is limited to monocytes and macrophages. CD14 is a glycosyphosphatidylinositol (GPI)-anchor membrane-associated protein which lacks transmembrane and intracellular domains. Its role consists in transfer of the LPS-LBP complex to TLR4 where LPS recognition is facilitated by another accessory co-receptor MD-2. MD-2 is physically associated with TLR4 and enhances its activation by alleviating the TLR4 oligomerization (Guha and Mackman 2001) (Dobrovolskaia and Vogel 2002).

Membrane activation of CD14/TLR4/MD2 receptor complex triggers further signaling through cytoplasmic TIR domain, where intracellular adaptors proteins are recruited to induce further downstream effector protein (Figure 2). In dependence on the engaged adaptor protein two main pathways are distinguished: myeloid differentiation factor 88 (MyD88)-dependent pathway leading to production of pro-inflammatory cytokines and Toll/IL-1R domain-containing adaptor inducing interferon β (TRIF)-dependent pathway associated primarily with intracellular TLR3 (Yoshino, Chiba et al. 2014). TRIF is activated during viral infection stimulates production of interferon β via activation of interferon regulatory factor 3 (IFR-3) (Mandrekar and Szabo 2009, Yoshino, Chiba et al. 2014). Nowadays, three other adaptor proteins, except MyD88 and TRIF, have been described: MAL (also known as TIRAP), TRAM and SARM. In TLR4 signaling MAL adaptor protein bridges TIR domain and MyD88 in order to diminish electrostatic surface charges between these proteins and therefore facilitates their connection. Upon TLR engagement, oligomeric receptor-associated complex termed Myddosome is formed. This tower shaped assembly, stabilized by specific death domain interactions, contains dimers of MyD88s linked to serine/threonine kinases, the IL-1 receptor associated kinases (IRAKs). First, likely the most important IRAK for transducing positive signal, IRAK4 interacts with MyD88 followed by autophosphorylation and recruitment of IRAK1 or IRAK2 (De Nardo 2015).

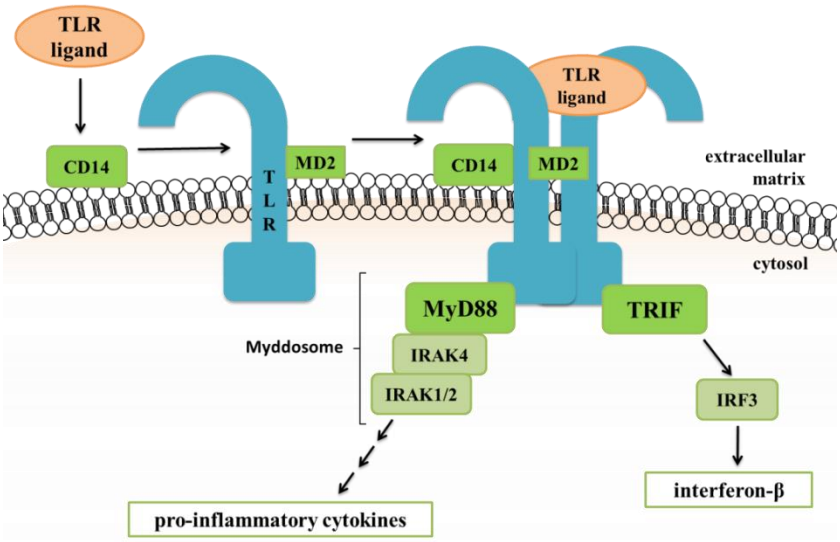

Figure 2: Toll-like receptor activation and recruitment of adaptor proteins.

IRAKM (also known as IRAK3) compared to all mentioned IRAKs, is believed to act predominantly as negative regulator of signal transduction by potentially inhibiting the dissociation of IRAKs with subsequent adapter TNF receptor-associated factor 6 (TRAF6) from the TLR receptor complex. TRAF6, an E3 ubiquitin ligase, catalyzes ubiquitin transfer to succeeding downstream proteins (De Nardo 2015).

4.1.3 Signaling pathway leading to activation of the nuclear factor κB

Rapid-acting primary transcription factor NFκB is the pivotal regulator of cell survival genes including also regulation of inflammatory or stress response, differentiation and proliferation. Diverse harmful stimuli (e.g. resctive oxygene species (ROS), TNFα, IL-1β, LPS) launch NFκB translocation into the nucleus, DNA binding via shared Rel domain and promote subsequent gene transcription of multiple cytokines, chemokines, adhesion molecules and enzymes. ReIA (p65), ReIB, c-Rel, NFκB1 (p105/p50) and NFκB2 (p100/p52) are members of NFκB protein family retained in the cell cytoplasm in dimeric form inhibited by κB subunit. For inflammatory response via TLRs, the classical pathway is fundamental (Figure 3), comprising p65/p50 heterodimer as a predominant combination. Upon activation κB inhibitory protein is first phosphorylated by IKK complex consisting of IKKα/IKKβ/NEMO subunits. Once phosphorylated, IκB undergoes ubiquitination and subsequent degradation by the proteasome (Luo, Kamata et al. 2005, Hayden and Ghosh 2008).

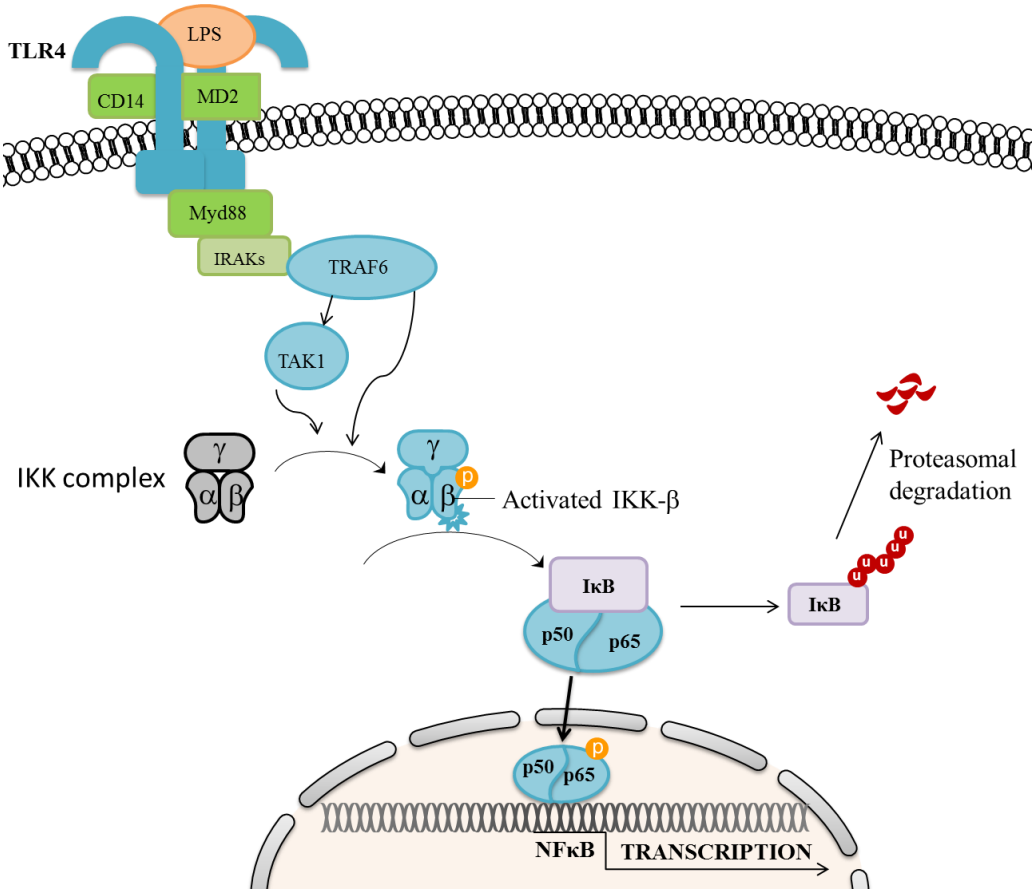

Figure 3: NFκB classical signaling pathway.

4.1.4 Mitogen-activated protein kinase signaling pathway

Extracellular receptor activated kinase (ERK), p38 and c-jun-NH_2-terminal kinase (JNK) are crucial members of MAPK cascades implicated in various vital-determing cellular process including proliferation, differentiation, apoptosis or survival. Besides, they are important regulators of inflammatory responses in immune cells since their engagement results in phosphorylation of transcriptional factor families such as Elk-1, AP-1, CREB regulating translation of diverse genes encoding inflammatory, cell survival and apoptotic mediators. Each MAPK exists in several isoforms. There are 3 recognized isoforms of JNK – JNK1, JNK2 present in most of the tissues and JNK3 which expression is limited to neuronal cells, heart and testes. In the case of p38, 4 isoforms (α, β, γ and δ) have been described to date. ERK includes 8 isoforms of which ERK1 and ERK2 are considered as the dominant ones (Kim and Choi 2015).

MAPKs are serine/threonine kinases activated by their upstream MAPK kinases (MAPKK) which were previously phosphorylated by their MAPKK kinases

(MAPKKK) activated by GTPases such as Ras or Rho family GTPases as an reaction to multiple, especially deleterious, impulses (Figure 4) (Kim and Choi 2015).

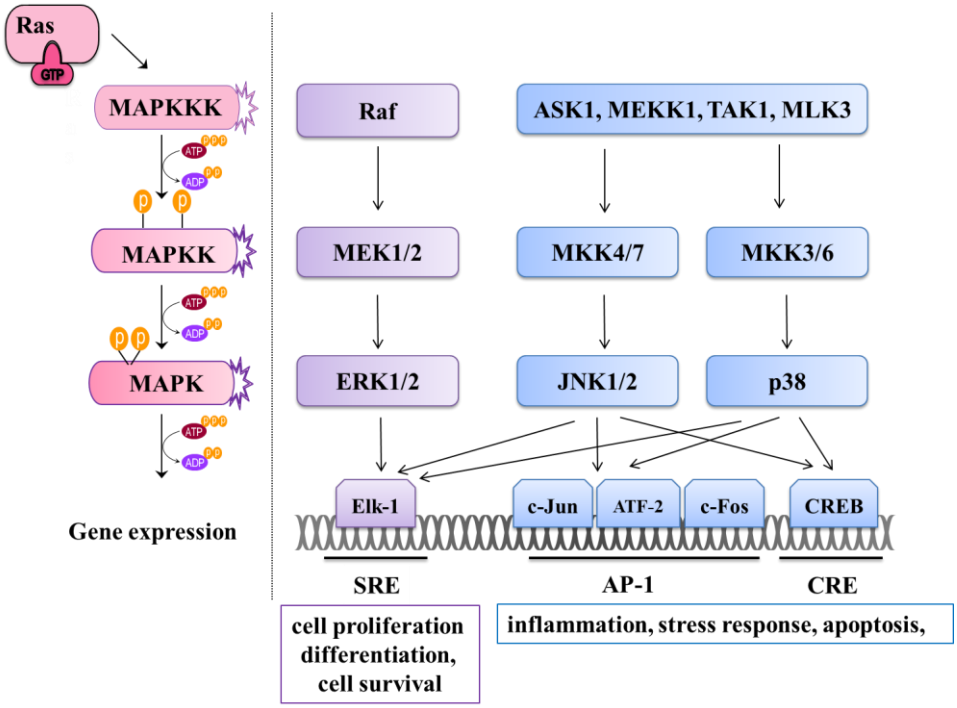

Figure 4: Summary of mitogen-activated protein kinase cascade.

At least 20 various MAPKKKs which phosphorylate 7 MAPKKs have been described (Johnson and Nakamura 2007). Some of them are specific for concrete kinase or stimulus, the remaining are capable to activate diverse downstream kinases and possess overlapping stimuli. Moreover, further regulation is provided by scaffolds proteins. This diversity allows integration and regulation of MAPK cascades in response to wide spectrum of external and also endogenous stress signals (Kim and Choi 2015).

Main ERK1/2 upstream kinases are MEK1 and MEK2 that are phosphorylated by their MAPKKKs c-Raf, activated by Ras. In contrast to the others MAPK, ERK sensed by growth factors could be considered as housekeeper regulator, involved primarily in cell differentiation, proliferation or cell survival. On the other hand, p38 and JNK are activated mainly by danger signals (e.g. cytokines, oxidative or ER stress) and regulate stress response. P38 is activated by MKK3 and 6 activated by MKKKs like ASK1, MEKK1, TAK1 or MLK3. MKK4 and MKK7 are considered to be direct

activators of JNK and can be activated by the same MKKs that act in p38 pathway. Ultimately, both of these pathways lead to activation of transcriptional factor such as c-Jun, ATF-2, c-Fos managing inflammatory response as well as CREB, Bcl-2 or Bad involved in apoptotic regulation (Swantek, Cobb et al. 1997, Johnson and Nakamura 2007, Sabio and Davis 2014, Kim and Choi 2015).

4.1.5 Involvement of cyclooxygenase-2 and inducible nitric oxide synthetase in Toll-like receptor 4 signaling pathway

Cyclooxygenase-2 (COX-2) is an inducible enzyme expressed in many cell types including monocytes and macrophages when stimulated by cytokines, endotoxins, growth factors, phorbol esters or oncogenes. COX-2 catalyzes conversion of arachidonoic acid to pro-inflammatory prostaglandins (mainly prostaglandin-E2, PGE2) and therefore plays an important role in inflammation. Transcription factor necessary for COX-2 expression are AP-1 activated by MAPK as well as NFκB (Hwang 2001, Korbecki, Baranowska-Bosiacka et al. 2013).

Nitric oxide (NO) is important signaling molecule acting in many physiological and pathological process synthetized by various isoforms of enzyme called nitric oxide sythetase (NOS). For example, known also as endothelium-derived relaxing factor plays an important role in vasodilation and therefore regulation of blood flow. However, when over-produced by immune cells by inducible NOS (iNOS) it becomes a dangerous free radical molecule involved in propagation and impaired regulation of inflammatory response (Kleinert, Schwarz et al. 2003). COX-2 and NO pathways are close-knit: NO enables to activate COX-2 expression and PGE2 generated by COX-2 negatively regulates expression of iNOS (Blazovics, Hagymasi et al. 2004). And both of them may be induced by LPS via TLR4 (Wasserman 2000).

4.2 Ursodeoxycholyl lysophosphatidylethanolamide

4.2.1 Bile acids, structure and biological activity relationship

Primary BAs (cholic acid (CA) and deoxycholic acid (DCA)) are synthetized in the hepatocytes from cholesterol and they can be later dehydroxylated by microbial flora in the colon to secondary (chenodeoxycholic acid (CDCA) and litocholic acid

(LCA)). Further epimerization in the liver gives rise to tertiary BAs, including ursodeoxycholi acid (UDCA) (Poupon 2012, Centuori and Martinez 2014). After synthesis bile acid are conjugated with amino acids – glycine or taurine and actively secreted and stored in the gallbladder from where they are excreted after dietary fat intake. Enteric hormones – cholecystokinin and secretin, regulates their release into the duodenum where they accomplish their main physiological role – emulsification and solubilization of lipids and lipid soluble vitamin and their further transport in hydrophilic environment. Moreover, BAs function also as signaling molecules through membrane receptor (TGR5) or even nuclear receptor such as farnesoid X receptor (FXR). In the ileum 95% of BAs is reabsorbed and transported back to the liver by portal vein. The rest of them reach the colon where they are deconjugated and subsequently converted by intestinal bacteria to secondary BAs or excreted by feces (Centuori and Martinez 2014, Jones, Alpini et al. 2015).

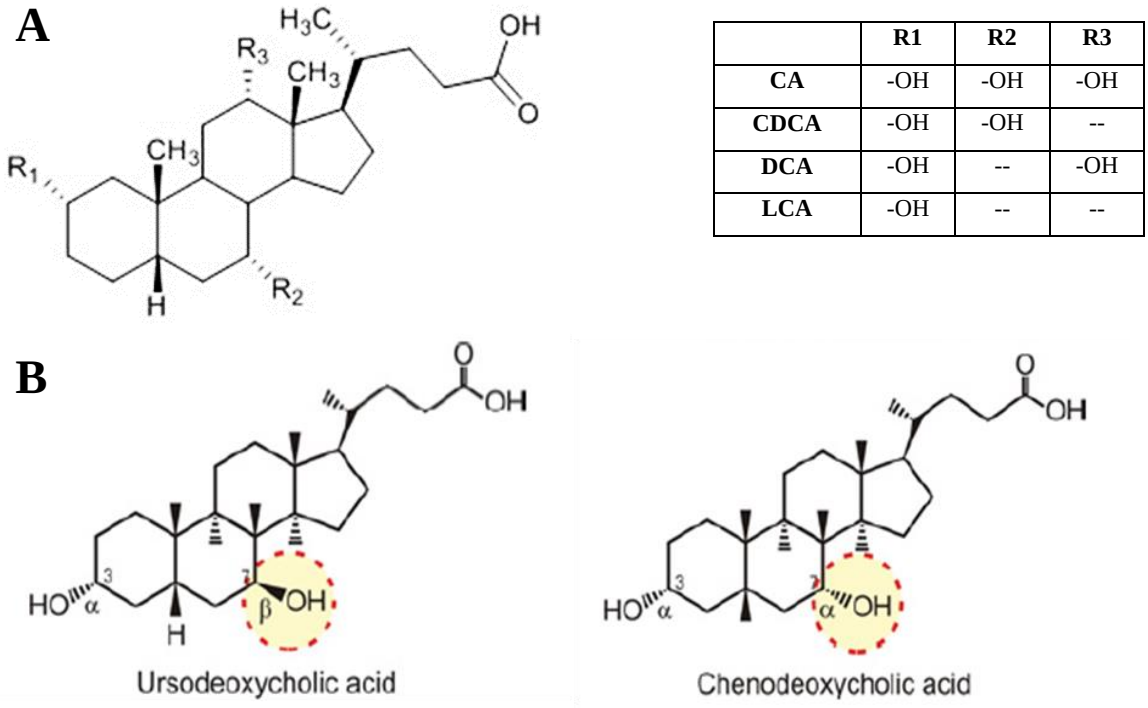

	R1	R2	R3
CA	-OH	-OH	-OH
CDCA	-OH	-OH	--
DCA	-OH	--	-OH
LCA	-OH	--	--

Figure 5: (A) chemical structure of β-cholanic acid, and the structure of bile acid indicated in the table. **(B)** The comparison of structure of protective ursodeoxycholic acid (3α,7β-dihydroxy5β-cholanoic acid) and cytotoxic isomer chenodeoxycholic acid (3α,7α-dihydroxy-5β-cholanoic acid) (Roma et al. 2011).

UDCA, as well as all bile acids are 24-carbon steroids, 5β-cholanic acid derivatives and differ on each other with the number and orientation of the hydroxyl groups Figure 5A. BAs are amphiphilic molecules and their biological characteristics

are largely dependent on their hydrophobic/hydrophilic ratio consequent from their chemical structure. The hydrophility of BAs increases with subsequent structure modifications (Figure 6):

1. Taurin conjugates are more soluble in the water
2. With increasing number of hydroxyl groups
3. Epimerization of the hydroxyl group in the 7C-position, equatorial position increases hydrophilicity (Roda, Minutello et al. 1990, Poupon 2012)

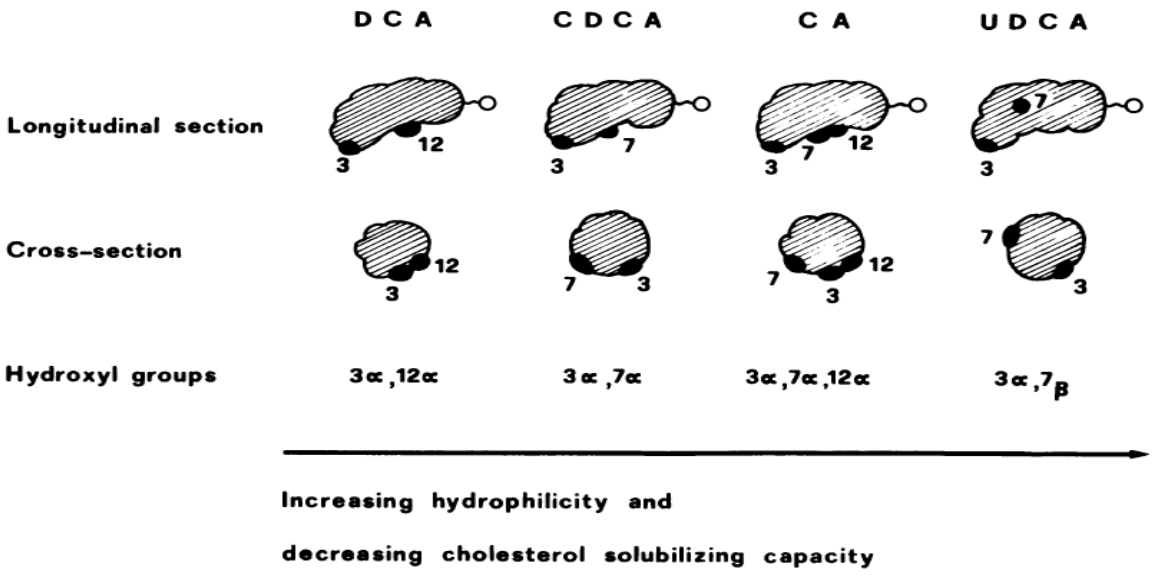

Figure 6: Relationship between structure and characteristics of different bile acids (Roda, Minutello et al. 1990).

Ensuing from these criteria, CDA and CDCA are classed as hydrophobic BAs whereas CA and UDCA are considered as hydrophilic (Figure 5B). Hydrophobic BAs are cytotoxic, inflammagen and immunosuppressive and play an important role in pathogenesis of different diseases including cholangiopathies and cancer. The importance of their toxicity accrue while their accumulation during cholestasis and may cause liver hypertrophy ultimately leading to the liver failure (Poupon 2012).

4.2.2 Therapeutic use of ursodeoxycholic acid

In traditional Chinese medicine, drug called “shorea spp.” acquired from bear bile was used in a treatment of hepatobiliary diseases for many centuries (Guarino, Cocca et al. 2013). Ursodeoxycholic acid (UDCA) originally isolated from bear bile, is

nowadays successfully used in a non-surgical treatment of cholesterol gallbladder stones (Stokes, Gluud et al. 2014), primary biliary cirrhosis (PBC) (Zhu, Shi et al. 2015), primary sclerosing cholangitis (PSC) (Zhu, Shi et al. 2015) and likely would/will be effective in the therapy of non-alcoholic fatty liver disease (NAFLD) (Poupon 2012). UDCA is an endogenous bile acid (normally comprises approximately 3% of human bile) (Kotb 2012) possessing not only hepatoprotective therapeutic properties but exhibit also anti-inflammatory, chemoprotective characteristics and anti-apoptotic by reducing ER stress, ROS production and influencing mitochondrial cell-death pathway. Its versatility can be used also to treat non-hepatic: neurodegenerative diseases (e.g. Alzheimer, Parkinson or Huntington), diabetes or obesity, where improving insulin resistance. Its anti-inflammatory properties can be used in therapy of autoimmune diseases such as inflammatory bowel diseases and its protective effects can put into effect in the treatment of renal injury, retinal disorders or stroke (Vang, Longley et al. 2014).

4.2.3 Ursodeoxycholyl Lysophosphatidylethanolamide

A phospholipid conjugate, ursodeoxycholyl lysophosphatidylethanolamide (UDCA-LPE) (Figure 7) was synthetized by Chamulitrat research group as a new therapeutic approach for the treatment of NASH where the effective therapy is still missing on the basis of following) different concepts:

1. The level of phosphatidylcholine (PC), the main cellular phospholipid, is depreciated during NASH and plays an important role in its pathogenesis (Li, Agellon et al. 2006). However, substitution of PC has no effect on liver fibrosis in patients with alcoholic steatohepatits, indicating that PC is not effectively taken up by hepatocytes. Lysophosphatisylethanolamide (LPE) is a lyso-form of phosphatidylethanolamine (PE). LPE should be an adequate precursor of PC based on presumptions that lysophopholipids are more easily taken up by cells and afterwards (Chamulitrat, Burhenne et al. 2009). This statement is supported by the study, where UDCA-LPE has shown superior efficacy in liver injury protection than UDCA-PE (Pathil, Warth et al. 2012). LPE is easily converted in cytoplasm by PE-methyltrasferase (PEMT) to PC (Chamulitrat, Burhenne et al. 2009).

2. UDCA can be used as specific carrier of targeting LPE to hepatocytes seeing that as a bile acid is taken up by/in the liver. This liver-targeting capability was already used to deliver nitric oxide donors (Fiorucci, Antonelli et al. 2001). Moreover, UDCA alone was anticipated to be beneficial in the therapy of NASH due to its cytoprotective effects (Xiang, Chen et al. 2013). These assumptions made UDCA an ideal ligand for coupling with LPE.
3. For this purpose, UDCA-LPE would be after delivery to hepatocytes hydrolyzed to UDCA and LPE.

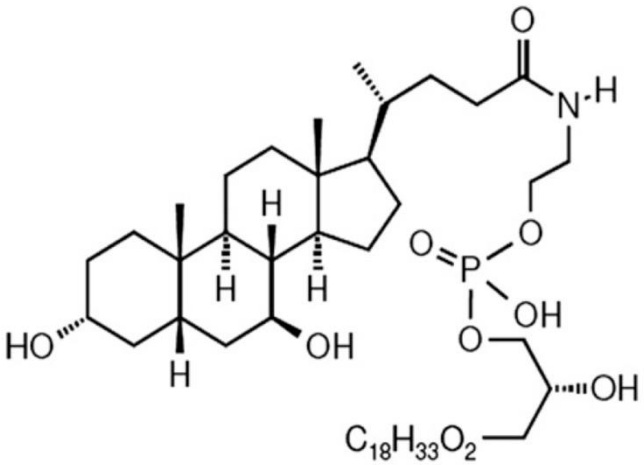

Figure 7: Structure of UDCA-LPE (Chamulitrat et al 2013).

Surprisingly, UDCA-LPE was not hydrolyzed as expected and moreover UDCA-LPE as intact molecule has manifested stronger protective effects on hepatocytes than UDCA, LPE or UDCA + LPE *in vivo* as well as *in vitro*. UDCA-LPE performed anti-apoptotic properties and is also able to interact with Akt and ERK pathway. Cytoprotective characteristics of the bile acid conjugate may be explained on one hand by the physico-chemical effects of UDCA-LPE to stabilize plasma and mitochondrial membrane and on the other hand by the capacity of UDCA-LPE to interact with different receptors and therefore influence different signaling pathways (Chamulitrat, Burhenne et al. 2009). Further investigation has shown that UDCA-LPE is able to suppress TNFα-induced apoptosis and inflammation in hepatocytes in vitro and galactosamine/LPS-mediated hepatitis in mice (Pathil, Warth et al. 2011). Moreover, UDCA-LPE ameliorates steatosis, hyperlipidemia and inflammation in two murine model of NAFLD – high fat diet and methionine-choline-deficient diet (Pathil, Mueller et al. 2012). This bile-salt phospholipid conjugate also exhibits anti-hepatofibrotic properties (Pathil, Mueller et al. 2014).

5 AIM OF THE STUDY

UDCA-LPE is a cytoprotective drug designed by Chamulitrat research group as a new potential approach in NAFLD treatment. It exhibits strong anti-inflammatory effects in various experimental murine models of liver injury.

The aim of this study is to identify signaling molecules affected by UDCA-LPE during an induction of inflammatory response by bacterial product LPS in human THP-1-derived macrophages. LPS produced by gut bacteria is potent agonist of TLR4 and therefore LPS-induced inflammation in macrophages will be adequate model for this study.

For this purpose, ELISA will be used to determine release of pro-inflammatory cytokines TNFα, IL-6 and IL-1β. Subsequently, indirect immunofluorescence will be performed to investigate nuclear translocation of phosphorylated transcription factors encompassed in inflammatory response – NFκB, c-Jun, ATF-2. Expression of MAPK signaling pathway will be assessed by Western blot analysis.

In addition, I will aim to isolate lipid raft in order to assess recruitment of adaptor protein MyD88 and TRAF6 into the lipid rafts. Consequently, I will evaluate the ability of UDCA-LPE to influence association of these adaptor proteins with TLR4 and therefore modulate subsequent downstream signaling.

6 MATERIALS AND REAGENTS

6.1 Materials

6.1.1 Devices

In the table below (Table 2), the list of devices used in this study is provided.

Device	Manufacturer
+4 °C refrigerator, FKU 1800	Liebherr (Bulle, Switzerland)
-20 °C freezer, MedLine	Liebherr (Bulle, Switzerland)
-80°C freezer, Hera Freeze HFU B Series	Thermo Scientific (Waltham, USA)
analytical balance, 2001 MP 2	Sartorius (Göttingen, Germany)
analytical balance, EMB 600-2	Kern (Balingen, Germany)
cell culture hood, HERAsafe	Thermo (Darmstadt, Germany)
cell culture incubator, HERAcell	Thermo, Darmstadt, Germany)
centrifuge, 5415 D	Eppendorf (Hamburg, Germany)
centrifuge, Biofuge fresco	Heraeus Instruments (Hanau, Germany)
centrifuge, Rotina 35R	Hettich Lab Technology (Tuttlingen, Germany)
crushed ice maker, AF 20	Scotsman (Ipswich, UK)
electrophoresis power supply, PowerPac Basic	Bio-Rad Laboratories (Hercules, USA)
fume hood, Labcontrol	Trox Technik (Neukirchen-Vluyn, Germany)
heating block, HB-1	Wealtec (Sparks, USA)
heating block with air ventilation, Reacti-Therm III	Thermo Scientific (Waltham, USA)
magnetic stirrer and heating block, Ikamag Rec-G	IKA (Staufen, Germany)
mass spectrometer, Quattro micro API, Mircomass	Waters (Milford, USA)
microscope OLYMPUS AX70	Olympus (Hamburg, Germany)
miscroscope Axiovert 25	ZEISS (Ostfildern, Germany)
Neubauer improved hemocytometer	MARIENFELD (Lauda-Königshofen, Germany)
pH meter, pH 537 microprocessor	Wissenschaftlich-Technische Werkstätten (Weilheim, Germany)
rocker, mini see-saw rocker SSm4	Stuart (Stone, UK)
spectrophotometer, NanoDrop 2000	Thermo Scientific (Waltham, USA)
SW41TI rotor for ultracentrifuge	Beckman Coulter (Brea, USA)
ultracentrifuge, Optima XL-90	Beckman Coulter (Brea, USA)
vortex, Vibrax VXR	IKA (Staufen, Germany)
vortex, Vortex Genie 2	Scientific Industries (Bohemia, USA)
water bath, P14	Thermo Scientific (Waltham, USA
water ultra-purifier, TKA X-CAD	Thermo Scientific (Waltham, USA)

Table 2: List of all devices used in this work.

6.1.2 Tools and labware

All the tools and labware used in this research work is mentioned in the following table (Table 3).

Tool	Manufacturer
beaker, glass, graduated, 50, 100, 250 ml	Duran Group – Schott (Wertheim/ Main, Germany)
beaker, PP, graduated, 1000 ml	Brand (Wertheim, Germany)
electrophoresis transfer foam pads	Bio-Rad Laboratories (Hercules, USA)
bottle, for washing, PE-LD, 500 ml	Brand (Wertheim, Germany)
bottle, glass, graduated, autoclavable, 100, 500, 1000 ml	Duran Group – Schott (Wertheim/ Main, Germany)
box, carton, 10 × 10 pockets	Sarstedt (Nümbrecht, Germany)
comb, spacer, 10-, 15-well, Mini-Protean	Bio-Rad Laboratories (Hercules, USA)
forceps, for tissue, 1 × 2 teeth, 14 cm	Fine Science Tools (Heidelberg, Germany)
forceps, PTFE, 10 cm	Brand (Wertheim, Germany)
magnetic stir bar, PTFE, 30 mm	Brand (Wertheim, Germany)
pipet controller, Pipetboy acu	Integra Biosciences (Konstanz, Germany)
pipet, 12-channel ,Research plus 200 µl	Eppendorf (Hamburg, Germany)
pipet, glass, graduated, reusable, 10, 20 ml	Brand (Wertheim, Germany)
pipet, single channel, Research plus 2.5µl, 10 µl, 20µl, 100µl, 200µl, 1.000µl	Eppendorf (Hamburg, Germany)
X-Ray cassette, 20,3 cm × 25,0 cm	Kisker Biotech (Steinfurt, Germany)
plate, glass, for gel casting, 10.1 mm × 7.3 mm, Mini-Protean	Bio-Rad Laboratories (Hercules, USA)
plate, glass, spacer, for gel casting, 10.1 mm × 8.2 mm, Mini-Protean	Bio-Rad Laboratories (Hercules, USA)
tetra cell gel casting module, Mini-Protean	Bio-Rad Laboratories (Hercules, USA)
electrophoresis tetra companion running module, Mini-Protean	Bio-Rad Laboratories (Hercules, USA)
electrophoresis tetra electrode assembly, Mini-Protean	Bio-Rad Laboratories (Hercules, USA)
electrophoresis buffer tank and lid with power cables, Mini-Protean	Bio-Rad Laboratories (Hercules, USA)
electrophoresis transfer cell, Mini Trans-Blot	Bio-Rad Laboratories (Hercules, USA)
electrophoresis transfer module, Mini Trans-Blot	Bio-Rad Laboratories (Hercules, USA)
electrophoresis transfer mini gel holder cassette	Bio-Rad Laboratories (Hercules, USA)
electrophoresis transfer central core, Mini Trans-Blot	Bio-Rad Laboratories (Hercules, USA)

Table 3: List of all tools and labware used in this work.

6.1.3 Disposables

The table below (Table 4) includes the list of all disposable tools and material used in this work.

Product	Manufacturer
cell culture 6-, 12-, 24-well plate	Corning Incorporated (Corning, USA)
cell culture dish à 35×10 mm, 60×15 mm, Cellstar	Greiner Bio-One (Kremsmünster, Austria)
cell culture dish à 94×16 mm, FALCON®	Becton Dickinson (Franklyn Lakes, USA)
cell culture flasks T-25, T-75, T-160	Greiner Bio-One (Kremsmünster, Austria)
cell culture tubes à 15 ml, 50 ml, Cellstar	Greiner Bio-One (Kremsmünster, Austria)
Cell scrappers	Greiner Bio-One (Kremsmünster, Austria)
cryovials à 2 ml, Cryos	Greiner Bio-One (Kremsmünster, Austria)
foil, aluminium	Carl Roth (Karlsruhe, Germany)
foil, for sealing, Parafilm	Bemis (Oshkosh, USA)
gloves, Touchntuff Nitrile 92-600	Ansell (Yarra City, Australia)
microscope cover glasses à10 mm, 12 mm	MARIENFELD (Lauda-Königshofen, Germany)
Microscope slides, 76×26×1 mm	MARIENFELD (Lauda-Königshofen, Germany)
needle, sterile Microlance 25G	Becton, Dickinson (Franklyn Lakes, USA)
pipet tip micro, Ultratip 0.5 µl – 20 µl	Greiner Bio-One (Kremsmünster, Austria)
pipet tip, Ultratip 10 µl – 200 µl, 100 µl – 1000 µl	Greiner Bio-One (Kremsmünster, Austria)
pipet, sterile, costar Stripette, 5, 10, 25 ml	Corning Incorporated (Corning, USA)
plate, 96-well	SPL Life Sciences (Pocheon-Si, South Korea)
syringe, sterile Plastipak 1 ml	Becton, Dickinson (Franklyn Lakes, USA)
ultra-clear tubes for ultracentrifuge 14×98 mm	Beckman Instruments (Brea, USA)
test tube, micro, graduated, 0.2 ml, 1.5ml, 2ml	Sarstedt (Nürnbrecht, Germany)
transfer pipette, sterile	Sarstedt (Nürnbrecht, Germany)

Table 4: List of all disposables used in this work.

6.1.4 Other products

Other products used in this study are mentioned in the following table (Table 5).

Product	Manufacturer
blotting membrane, PVDF (polyvinylidene difluoride), Immobilon-P	Merck (Darmstadt, Germany)
ECL (enhanced chemiluminescence) film, Amserham Hyperfilm	General Electric Healthcare (Solingen, Germany)

Table 5: List of other products used in this work.

6.2 Reagents

In the following table (Table 6), the list of all reagents used performing this research work is provided. Chemicals marked with * were stored at 4 °C, the ones marked with ** were stored at -20 °C, the ones without mark were stored at room temperature (15-25 °C).

Product	**Manufacturer**
2-propanol, ≥ 99.8 %	Sigma-Aldrich (St. Louis, USA)
acetone	Sigma-Aldrich (St. Louis, USA)
ammonium chloride	Merck (Darmstadt, Germany)
APS (Ammonium persulfate)	Sigma-Aldrich (St. Louis, USA)
BioRad protein assay kit	Bio-Rad Laboratories (Hercules, USA)
BPB (Bromphenol blue)	Sigma-Aldrich (St. Louis, USA)
BSA (Bovine serum albumin)*	Sigma-Aldrich (St. Louis, USA)
BSA Standard	Sigma-Aldrich (St. Louis, USA)
chloroform, HPLC grade, ≥ 99.9 %	Merck (Darmstadt, Germany)
citric acid monohydrate	AppliChem (Darmstadt, Germany)
disinfectant, antifect N liquid	Schülke & Mayr (Nordersted, Germany)
disinfectant, Bacillol plus	Bode Chemie (Hamburg, Germany)
DMSO dimethylsulfoxid	AppliChem (Darmstadt, Germany)
DTT (dithiothreitol)	Sigma-Aldrich (St. Louis, USA)
ELISA MAX™ IL-6, Deluxe IL-1β	BioLegend, San Diego, USA
Entellan® mounting medium	Merck Millipore (Billerica, USA)
ethanol, ≥ 99.8 %	Sigma-Aldrich (St. Louis, USA)
FBS**	Gibco® (Darmstadt, Germany)
formaldehyde 37%	Sigma (Steinheim, Germany)
gelatin*	Sigma-Aldrich (St. Louis, USA)
glycerol anhydrous	AppliChem (Darmstadt, Germany)
glycine	AppliChem (Darmstadt, Germany)
ß-Glycerophosphate*	Sigma-Aldrich (St. Louis, USA)
hydrochloric acid, ACS reagent, 37%	Sigma-Aldrich (St. Louis, USA)
LPS from Escherichia coli 055:B5**	Sigma (Steinheim, Germany)
MeOH (methanol), ≥ 99.8 %	Sigma-Aldrich (St. Louis, USA)
MeOH (methanol), HPLC grade, ≥ 99.9 %	Sigma-Aldrich (St. Louis, USA)
ß-Mercaptoethanol*	Bio-Rad Laboratories (Hercules, USA)
milk, powdered, blotting grade	Carl Roth (Karlsruhe, Germany)
Mowiol-488, water-compatible mounting medium	Sigma-Aldrich (St. Louis, USA)
MTT**	Sigma-Aldrich (St. Louis, USA)
Optiprep™*	Axis-Shield POC AS (Oslo, Norway)

Product	Manufacturer
PageRuler, Protein Prestained Ladder	Thermo Fisher Scientific (Waltham, USA)
Penicillin**	Thermo Fisher Scientific (Waltham, USA)
phosphate buffered saline (PBS), pH 7.4, 10 ×	Life Technologies (Carlsbad, USA)
PMA**	Sigma (Steinheim, Germany)
PMSF (phenylmethanesulfonyl fluoride)	Sigma-Aldrich (St. Louis, USA)
Polyacrylamide 40%	Sigma-Aldrich (St. Louis, USA)
Poinceau S solution, 0.1% (w/v) in 5% acetic acid	Sigma-Aldrich (St. Louis, USA)
Protease Inhibitor Cocktail Set III	#539134, Calbiochem, (Darmstadt, Germany)
SDS (sodium dodecyl sulfate)	E. A. Thomas (Heidelberg, Germany)
sodium chloride (NaCl)	Sigma-Aldrich (St. Louis, USA)
sodium fluoride (NaF)	Sigma-Aldrich (St. Louis, USA)
sodium orthovanadate (Na_3VO_4)**	Sigma-Aldrich (St. Louis, USA)
Streptomycin**	Thermo Fisher Scientific (Waltham, USA)
Sulfuric acid (H_2SO_4) (95.0-98.0%)	Sigma-Aldrich (St. Louis, USA)
TEMED (tetramethylethylenediamine)	Sigma-Aldrich (St. Louis, USA)
TMB Substrate Set	BioLegend, (San Diego, USA)
Tris (2-amino-2-hydroxymethyl-propane-1,3-diol)	Carl Roth (Karlsruhe, Germany)
Triton X-100	Sigma-Aldrich (St. Louis, USA)
Trypan blue	Sigma (Steinheim, Germany)
Tween 20®	Sigma-Aldrich (St. Louis, USA)
UDCA-LPE (ursodeoxycholyl lysophosphatidylethanolamine)*	ChemCon (Freiburg, Germany)
Western blot, HRP substrate, Luminata Forte	Merck (Darmstadt, Germany)

Table 6: List of chemicals, solution and kits used in this work.

6.2.1 Primary antibodies for Western blot analysis

In the following table (Table 7) the list of all primary antibodies used for Western blot analysis is provided. Subsequent specification including origin, clonality, molecular weight, dilution and information about manufacturer are also documented in this table.

Target protein	Description (isotype - IgG, clonality)	Molecular weight, kDa	Dilution used	Manufacturer information (catalogue number, company)
COX-2	Rabbit, monoclonal	74	1:1.000	#12282, Cell Signaling, (Frankfurt am Main, Germany)
iNOS	Mouse, monoclonal	130	1:2.000	610431, Becton Dickinson (Franklin Lakes, New Jersey, USA)
Phospho-p44/42 MAPK (Erk1/2)	Mouse, monoclonal	42, 44	1:1.000	#9106 Cell Signaling, (Frankfurt am Main, Germany)

Target protein	Description (isotype - IgG, clonality)	Molecular weight, kDa	Dilution used	Manufacturer information (catalogue number, company)
Phospho-SAPK/JNK	Rabbit, monoclonal	46, 54	1:2500	#4668, Cell Signaling, (Frankfurt am Main, Germany)
Phospho-p38	Rabbit, monoclonal	43	1:1000	#9212, Cell Signaling, (Frankfurt am Main, Germany)
Phospho MKK-7	Rabbit, polyclonal	48	1:500	#4171, Cell Signaling, (Frankfurt am Main, Germany)
Phospho-SEK1/MKK-4	Rabbit, polyclonal	46	1:500	#9151, Cell Signaling, (Frankfurt am Main, Germany)
Phospho-c-Jun	Rabbit, monoclonal	48	1:500	#9261, Cell Signaling, (Frankfurt am Main, Germany)
c-Jun	Rabbit, monoclonal	39	1:500	ab40766, abcam, (Dresden, Germany)
Phospho ATF-2	Rabbit, monoclonal	70	1:500	#9221, Cell Signaling, (Frankfurt am Main, Germany)
β-actin	Mouse, monoclonal	43	1:10.000	Sigma-Aldrich (St. Louis, USA)
GAPDH	Rabbit, monoclonal	37	1:20.000	#2118, Cell Signaling, (Frankfurt am Main, Germany)
Flotilin-2	Mouse, monoclonal	42	1:2.000	610383, Becton Dickinson (Franklin Lakes, New Jersey, USA)
calnexin	Goat, polyclonal	90	1:500	Sc-6465, Santa Cruz Biotechnology, (Heidelberg, Germany)
Myd88	Rabbit, monoclonal	33	1:1.000, 1:500	#6483, Cell Signaling, (Frankfurt am Main, Germany)
TRAF6	Rabbit, polyclonal	60	1:500	Sc-7221, Santa Cruz Biotechnology, (Heidelberg, Germany)

Table 7: List of primary antibodies used for Western blot analysis used in this work.

6.2.2 Secondary antibodies (HRP-conjugated) for Western Blot

In the following table (Table 8) the list of all secondary antibodies used for Western blot analysis is provided. Subsequent specification including specifity, origin, dilution range and information about manufacturer are also documented in this table.

specifity	origin	Range of the used dilution	Manufacturer information (catalogue number, company)
anti-mouse	goat	1:5.000 – 1:15.000	#sc-2005, Santa Cruz Biotechnology, (Heidelberg, Germany)
anti-goat	donkey	1:5.000	#sc-2020, Santa Cruz Biotechnology, (Heidelberg, Germany)
anti-rabbit	goat	1:5.000 – 1:10.000	#7074S, Cell Signaling, (Frankfurt am Main, Germany)

Table 8: List of secondary antibodies used in Western blot.

6.2.3 Antibodies and fluorescence stain used for immunofluorescence

In the table below (Table 9) the list of all antibodies and fluorescent dyes used for immunofluorescence is provided. Subsequent specification including origin, dilution and information about manufacturer are also documented in this table.

specifity	origin	Dilution used	manufacturer
NFκB, p65	rabbit	1:200	#8242, Cell Signaling, (Frankfurt am Main, Germany)
P-ATF-2	rabbit	1:50	#9221, Cell Signaling, (Frankfurt am Main, Germany)
P-c-Jun	rabbit	1:100	#9261, Cell Signaling, (Frankfurt am Main, Germany)
AlexaFluor® 488	goat anti rabbit	1:100	A11034, life technologies, (Eugene, OR, USA)
Rhodamine	donkey anti-rabbit	1:100	sc-2095, Santa Cruz Biotechnology, (Heidelberg, Germany)
DAPI	-	1:200	Sigma-Aldrich (St. Louis, USA)
Phalloidin CruzFluor™ 488	-	1:1000	Sc-363791, Santa Cruz Biotechnology, (Heidelberg, Germany)

Table 9: List of antibodies and fluorescence staining used while performing immunofluorescence.

6.3 Software

In the table below (Table 10), the list of software used in this study is provided.

Software	Manufacturer
Microsoft Office	Microsoft Corporation, (Redmond, USA)
Image J	public domain
Graph Pad Prism 5.0	Grappa Software, (La Jolla, USA)
ChemDraw	PerkinElmer, (Waltham, USA)
Cell^{F} software	Olympus, (Hamburg, Germany)

Table 10: List of software used un this study.

6.4 Methods

6.4.1 Cell culture

Human primary monocytes isolated from 1-year old male with acute leukemia, THP-1 cell line (purchased from Cell Lines Service) was kindly provided by Assist. Prof. Dr. Warangkana Chunglok, Walailak University, Thailand. After thawing and removing freezing medium, cells were cultivated in suspension in RPMI medium 1640

supplemented with 10% of heat-inactivated foetal bovine serum (FBS) 100 U/ml penicillin (P) and 100 µg/ml streptomycin (S) at 37 °C in humid atmosphere of 5% CO_2. The medium was changed twice a week; cell suspension was centrifuged at 2,000 RPM for 4 minutes in Rotina 35 R centrifuge (Hettich, Tuttlingen, Germany), old medium was removed, cell pellet was re-suspended in a new medium preheated at 37 °C and transferred to a new flask.

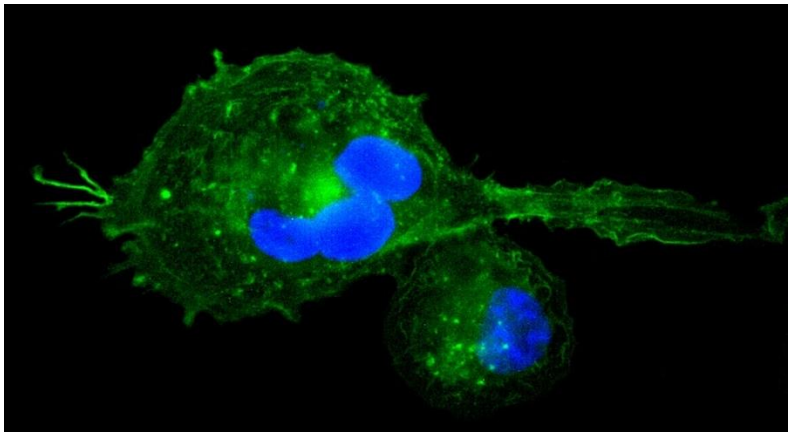

Figure 8: Differentiated THP-1, fixed in 4% formaldehyde, cytoskeleton - actin staining with Phalloidin CruzFluor 488, nuclear staining with DAPI. Magnification 100×.

Counting cells: In order to determine cell quantity and their viability, cells suspension (5 µl) was diluted with PBS (85 µl) and stained with 0,4% Trypan Blue in PBS (10 µl). Subsequently, 100 µl of this suspension was applied to the hemocytometer. Using 10× magnification of Axiovert 25 microscope (ZEISS, Ostfildern, Germany), live (unstained) cells were counted. Final amount of cells was calculated using following formula:

$$\frac{a+b+c+d}{4} \times D_f \times 10^4$$

where *a, b, c, d* stand for number of cells in 16-squares corner areas, D_f is dilution factor (volume of cells suspension/total volume of mixture put into the hemocytometer = 100 µl).

Differentiation: When needed, THP-1 monocytes were differentiated into macrophages incubating with 100 nM phorbol 12-myristate 13-acetate (PMA) for 72 hours at 37 °C.

Freezing cells: Cell suspension was centrifuged at 2,000 RPM for 4 minutes and re-suspend in the freezing medium (RPMI medium 1640 containing 20% FBS, 1% P/S and 20% glycerol as cryoprotective agent). Cells were counted in hemocytometer and diluted to final concentration 2×10^6 cells/ml. This cell suspension was transferred into cryogenic storage vials and frozen at /80 °C, afterwards in liquid nitrogen.

6.4.2 Preparation of whole cell lysate

Cell lysis buffer for Western blot analysis (kept at 4 °C, protease inhibitors were added freshly before use)

- 20 mM Tris-HCl (pH 7.4),
- 150 mM NaCl
- 10 mM $MgCl_2$
- 2 mM EDTA
- 10% glycerol
- 1% Triton X-100
- 2.5 mM β-glycerolphosphate
- 1 mM NaF
- 1 mM DTT
- Added when used:
    - 10 mg/ml PMSF in isopropanol – 10 µl/ml,
    - 100 mM Na_3VO_4 – 10 µl/ml,
    - Protease Inhibitor Cocktail set III – 12 µl/ml

The culture medium was discarded and cells were washed twice with cold PBS. Pre-chilled cell lysis buffer was added (10 µl/mm of diameter of a cell culture dish), cell culture dishes were placed on ice or in the cold room and incubated for 30 minutes on the rocker in slow speed. Next, cell lysate was scrapped and transferred into microcentrifuge tubes and at 13,000 RPM for 10 minutes at 4 °C. The supernatant was subjected to a protein analysis.

6.4.3 Protein assay

Principle: The concentration of proteins in samples was determined by the Bio Rad DC Protein Assay. It is a colorimetric, 2-step assay based on the reaction of protein in the sample with an alkaline copper tartrate solution and Folin reagent which lead to blue colour development due to reduction of Folin reagent by amino acids (Lowry, Rosebrough et al. 1951, Peterson 1979).

Procedure: The assay was performed in 96-well microplate in accordance to manufacturer´s instructions. Samples were diluted in the distilled water in the range 1:1 – 1:5 and BSA standard was diluted in 6 two-fold gradient dilution, distilled water was used as empty control. Reagent A* was prepared mixing 20 µl of Reagent S to each ml of Reagent A. 5 µl of the sample/standard was pipetted into the tested wells (in duplicate for samples, in triplicate for standard) followed by 25 µl of reagent A* and 200 µl of Reagent B. After 15 minutes, the absorbance was read at 750 nm. The protein concentration was calculated in Excel-Office.

6.4.4 Western blot analysis

Principle: The Western blot analysis is a method serving to specifically detect proteins in the sample. First, proteins are separated by different molecular weight performing SDS-Polyacrylamide gel electorphoresis (SDS-PAGE) and subsequently transferred to PVDF membrane where they are detected by immunobloting.

Buffers, solution and gels

- **3× Laemmli SDS-Sample Buffer:**
  - 125 mM $NaPO_4$ (pH 7.0)
  - 6% SDS (w/v)
  - 30% glycerol
  - 0.009% BPB
  - 10% β-mercaptoethanol
- **Running buffer:**
  - 25 mM Tris
  - 190 mM glycine
  - 0.1% SDS (w/v)
- **Transfer buffer**:
  - 20% MeOH
  - 25 mM Tris
  - 190 mM glycine
- **Washing buffer** = TBST (Tris-Buffered saline and Tween):
  - 50 mM Tris-Cl (pH 7.6)
  - 150 mM NaCl
  - 0.1 % Tween 20
- **Blocking buffer:** 5 % milk (w/v) in TBST
- **Buffer for primary antibody solution:** 5% BSA in TBST

- **Stripping buffer:**
    - 62.5 mM Tris
    - 1% SDS (w/v)
    - 100 mM β-mercaptoethanol
- **Gels:** Exact volume of reagents for making SDS-gels is comprised in Table 11. Particular component were added in order they are listed in the table. TEMED were added as very last.

Components	Amount in µl of the component used for two 0.75 mm or one 1.5 mm gel			
	8% gel	9% gel	10% gel	3% sacking gel
40% polyacrylamide	2000	2250	2500	750
1.5 M Tris-Cl, pH 8.8	2500	2500	2500	-
10% SDS (w/v)	100	100	100	100
0.5 M Tris–Cl, pH 6.8	-	-	-	2500
H_2O	5300	5050	4800	6550
10% APS (w/v)	100	100	100	100
TEMED	10	10	10	10

Table 11: Preparation of gels for SDS-PAGE electrophoresis.

Procedure

Preparation of samples: In order to normalize amount of proteins in samples for immunoblot analysis, the samples were equalized in protein content by adding the appropriate volume of Cell lysis buffer. Then, 3× Laemmli SDS-Sample Buffer was added, samples were vortexed and heated at 95°C for 5 minutes, centrifuged at maximal speed (13,000 RPM) for 5 minutes and kept in -20 °C until further use.

SDS-PAGE Electrophoresis: Equal protein quantity in the range of 20–40 µg was loaded on a 8–10% SDS-Polyacrylamide gel. Gels were run in BioRad chamber at amper constant 40 mA for around 1.5 hour for 2 gels and 50–60 mA for about 2 hours for 4 gels in Running buffer. To indicate molecular weight of protein the Thermo Scientific PageRuler Prestained Protein Ladder was used. For this purpose, protein marker was thaw at room temperature and loaded 5-10 µl per well.

Transfer of proteins: after electrophoretic separation, proteins were transferred to PVDF membrane. Prior to transfer, PVDF membrane was activated by dipping in cold methanol for 30 seconds and sponges and filter paper were pre-soaked in Transfer buffer. To prevent protein degradation caused by hot temperature, running chamber was kept in cool by providing the transfer in the cold room and using ice-blocks. Transfer was undertaken in Transfer buffer at 100 V for 1.5 hour. Afterwards, transferred

proteins were visualized by dipping the PVDF membrane into Poinceau S solution (Figure 9).

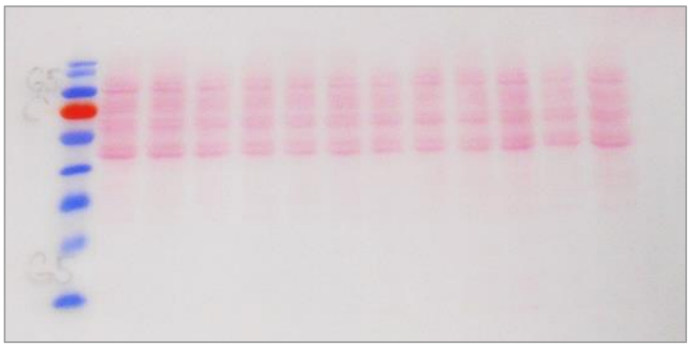

Figure 9: Visualization of transferred protein on PVDF membrane with Poinceau S.

Immunodetection. Membrane was blocked with 5% non-fat milk in TBST for 2 hours at room temperature, washed 4×5 minutes in TBST and incubated overnight (16–18 hours) at 4 °C with primary antibody using its adequate dilution in 5% BSA in TBST. The next day, membrane was washed 5×5 minutes in TBST, followed by incubation with secondary antibody with appropriate dilution in blocking buffer for 1hour at room temperature. Subsequently, membrane was washed 5×5 minutes in high speed on the rocker again in TBST and submitted to detection, starting with dipping in HRP Luminate forte solution, wrapping in saran wrap and transporting to X-ray cassette. Film was developed in the dark room.

Stripping: After detection, membranes were washed in TBST and stripped in Stripping buffer at 62 °C for 15–30 minutes. Then blots were washed in TBST, blocked in 5% milk and reprobed.

6.4.5 Immunofluorescence

Principle: Immunofluorescence is a biological, cell imaging technique combining the use of antibodies and fluorescent molecules allowing visualization and thereby detection of molecules of interest in cells and tissues. In direct immunofluorescence only single antibody connected directly to fluorophore and recognizing target antigen is used. In indirect immunofluorescence, first the cell or tissue being investigated are exposed to unconjugated antibodies for the target proteins molecules and subsequently to second anti-immunoglobulin antibodies linked with fluorescence dye such as fluorescin isothiocyanate (FTIC) or tetramethylrhodamine

isocyanate (TRITC). This provides both a visible signal and amplification of the signal and the results are observed with a fluorescence microscope (Donaldson 2015).

Procedure

Sample preparation: Cells were differentiated in 10 or 12 mm glass coverslips coated by gelatin. For this purpose, sterilized coverslips placed in the cell culture dishes were incubated with 0.1% gelatin in PBS for 1 hour at 37 °C. After removing the coating solution, coverslips were dried in open dishes for 30 minutes at room temperature. Afterwards, cells were seed in a 1.5×10^5 cells/ml density. After 72 hours of differentiation, the medium was discarded, coverslips were washed in PBS and treated.

Fixation in methanol: After treatment, the medium was removed and coverslips were washed twice with PBS. Cells were fixed in ice-cold methanol (pre-cooled at -20 °C) for 5-10 minutes followed by dipping into cold acetone for approximately 30 seconds. Next, coverslips were dried in air and frozen until further use.

To avoid unspecific binding of antibody, coverslips were treated at room temperature for 10 minutes with blocking buffer (1% BSA in PBST, PBS with 0.01 % Tween-20) and thereby permeabilized at the same time. After immersion in PBS, coverslips were incubated with primary antibody diluted to appropriate dilution in blocking buffer for 1hour followed by 1-hour incubation with 1:100 dilution in blocking buffer of Alexa Fluor 488 conjugated anti-rabbit IgG. Then cells were treated with DAPI (1:200 in blocking buffer) for 10 minutes. After precise washing, coverslips were mounted on glass slides with Entellan™, water-free mounting medium. Images were collected by OLYMPUS AX70 microscope (Olympus, Hamburg, Germany).

Fixation in formaldehyde: Cells were fixed with 4% formaldehyde in PBS for 15 minutes at room temperature. Then washed in PBS and incubated for 20 minutes at room temperature with 10 mM NH_4Cl in PBS to quench autofluorescence of the free aldehyde groups of the fixative solution. Coverslips were subjected immediately to analysis or kept in PBS at 4 °C for a few days until further use. Then, the same protocol as previously described was followed until the mounting step, where Mowiol-488 as water-compatible mounting medium was used.

6.4.6 MTT assay

Principle: MTT assay is versatile and quantitative colorimetric assay to determine viability of mammalian cells by measuring the activity of dehydrogenase enzymes. NAD(P)H-dependent cellular oxidoreductase enzymes in active mitochondria (present only in living cells) cleave the tetrazolium ring of MTT (3-(4,5-dimethylthiazol-2-yl)-2,5-diphenyltetrazolium bromide) to its insoluble formazan, which has a purple color. The development of the color is detected by spectrophotometer (Mosmann 1983).

Procedure: Cells after treatment was incubated overnight with new RPMI medium 1640 in presence of 10% FBS and 1% antibiotics (P/S). The next day, 20 µl of MTT solution diluted to guideline-recommended dilution from the stock solution to 0.2 mg/ml were added per well. After 4 hours of incubation at 37 °C in 5% CO_2 solution was removed and upraised formazan crystals were solubilized in 500 µl of DMSO. Solution was aliquoted to 96-well plate and absorbance was measured at 550 nm, the background was subtracted at 630 nm. Final calculations were realized in Excel.

6.4.7 Enzyme-linked immune sorbent assay, ELISA

Buffer preparation

- Coating buffer was prepared by adding 8.4 g $NaHCO_3$ and 3.56 g Na_2CO_3 to 1 l distilled water and adjusting to pH 9.5.
- Assay diluent 10% FBS were diluted in PBS
- Wash buffer contained 0.05% Tween-20 in PBS
- Stop buffer 1 M H_2SO_4
- Standard preparation: standard was reconstituted from lyophilizate in Assay Diluent and six two-fold dilution in Assay Diluent in duplicate was performed.

Procedure: For ELISA, protocols provided by the manufacturers were used. Each step was followed by excessive washing with 300 µl wash buffer for at least 4 times. For each incubation, plate was sealed with parafilm. One day prior to the experiments, 96 well plates were coated with capture antibody diluted in coating buffer and left to incubate at 4 °C overnight. The next day, plates were blocked with 200 µl of assay diluent in each well for 1 hour at room temperature with shaking. Then, 100 µl of

standard in duplicate, assay diluent as empty control and samples were added and incubated with shaking for 2 hours. A volume of 100 µl Detection antibody was added for 1 hour followed by 100 µl avidin-HRP for 30 minutes. As avidin-HRP is light sensitive this step was performed in the dark. For visualization, 100 µl TMB substrate was added and the plate was incubated in the dark for 10–30 minutes, dependent on color development. Finally, 100 µl of the Stop solution changed the reaction color from blue to yellow and the absorbance was measured immediately at 450 nm and subtracted at 570 nm on a micro plate reader. The amount of cytokine presented as pg/ml was calculated using Excel-software.

6.4.8 Lipid rafts isolation

Principle: Lipid rafts are highly organized microdomains composed of proteins and lipids floating freely in the bilayer of plasma membrane but have an ability to cluster to even higher organized dynamic assemblies. They are involved in multiple cellular processes by regulating membrane function, modulating membrane trafficking and signal transduction. Their lipid composition differs from other part of the membrane, because they are enriched in sphingophospholipids and cholesterol which tightly hold together. Moreover, they contain specific protein like caveolin. One of their characteristics is that they are insoluble in non-ionic detergent such as Triton X-100 at 4 °C. This become a tool for their isolation and give then acronym DRM standing for detergent resistant membrane (Simons and Ehehalt 2002, Pike 2003, Simons and Sampaio 2011). However, we must distinguish that DRM and lipid rafts are not exactly the same due to the artificial isolation at low temperature.

Procedure: DRM isolation was performed according to the procedure described by Ligwood et Simons (Lingwood and Simons 2007), but with modifications. THP-1 human monocytes were differentiated using 100n M PMA in 94 mm cell culture dish with seeding density 1×10^6 cells/ml for 72h. After treatment, attached cells were washed in PBS, followed by washing with TNE buffer (150 mM NaCl, 2 mM EDTA; 50 mM Tris-HCl, pH=7.4). Each following step was held in low temperature. Cells were scraped in 1.5 ml of TNE and centrifuged at 380 g for 5 minutes at 4 °C. Cell pellet was re-suspend in 800 µl TNE with protease inhibitor (Na_3VO_4 – 10 µl/ml, PMSF in isopropanol 10 µl/ml and Protease inhibitor cocktail III – 12 µl/ml) and homogenizes

with 25-G needle (25 stokes). To solubilize cell membrane, 720 µl of the cell homogenate was incubated with 80 µl of 10% Triton X-100 for 30 minutes with occasional wobble. The buffer concentration was adapted to 40% iodixanol (w/v) by mixing with 1600 µl of Optiprep (60% iodixanol). This mixture was transferred to centrifuge tubes overlayed with 4.8 ml of 30% iodixanol and 0.8 ml TNE buffer. Samples were centrifuged at 37,000 RPM (259,000 g) with SW41 rotor for 2 hours at 4 °C and separated into 7 fractions from the top to bottom and subjected to further analysis (Figure 10).

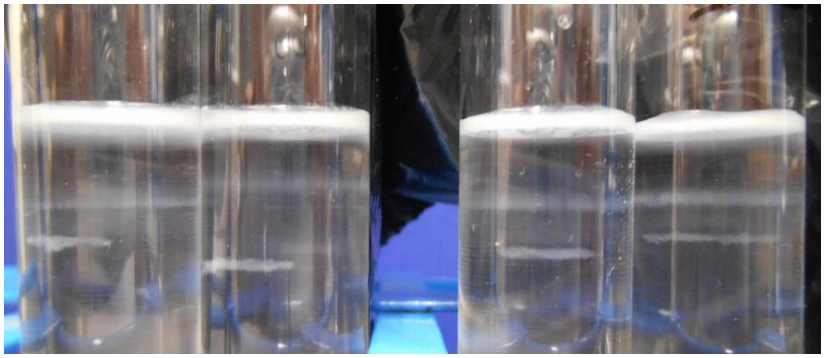

Figure 10: Floating lipid rafts after centrifugation at 259,000 g for 2 hours at 4 °C using SW41 rotor.

6.5 Statistical analysis

The number of experiments analyzed is indicated in the figures, all results were analyzed in GraphPad. Data are presented as mean ± SD.

If n<6, the results were evaluated by student´s t-test followed by unpaired test. For n≥6 firstly, the distribution was checked with Kolmogorov-Smirnov test (with Dallal-Wilkinson-Lilliefor P value). In case that the measured values passed normality test (α=0.05), the results were tested by 1 way ANOVA followed by Dunnet´s Multiple Comparison Test assuming Gaussian distribution.

7 RESULTS

7.1 Cytokine release and cell viability

Bacterial LPS is described as TLR4 agonist and strong inducer of the secretion of cytokines such as IL-6, IL-1β and TNF-α by immune cells – monocytes and macrophages. To examine anti-inflammatory properties of UDCA-LPE, the expression of afore-mentioned pro-inflammatory cytokines was determined by ELISA. For this purpose, differentiated THP-1 cells were pre-treated with increasing concentrations of UDCA-LPE in the range from 10 μM to 75 μM for 1 hour and subsequently treated with LPS (100 ng/ml) for 24 hours at 37 °C in humidified atmosphere of 5% CO_2. Cell viability was determined by MTT assay, the result is shown at Figure 11. The concentration of LPS used in this and also for all the others experiments is adequate to induce an expression of inflammatory mediators without killing them. Interestingly, UDCA-LPE significantly augments the metabolic activity of THP-1 cells.

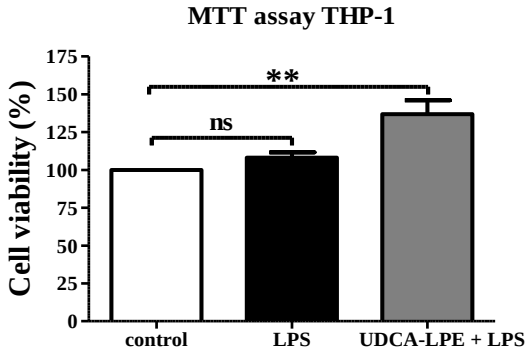

Figure 11: Cell viability, determined by MTT assay Cells were (or not) pre-treated with 50 μM UDCA-LPE, followed by LPS (100 ng/ml) incubation for 24 hours. Results are presented as mean ± SD from three independent experiments, **p<0.01 vs. control.

ELISA assay was performed using ELISA kits from BioLegend, protocols provided by manufacturer were followed as described in Materials and Methods. LPS treatment gives raise to strong production of TNFα, IL-6 as well as IL-1β. UDCA-LPE attenuates significantly the LPS-induced release of all of three inflammatory cytokines in dose-dependent manner (Figure 12). Therefore, to explore the molecular mechanism of this measurement, further experiments were submitted.

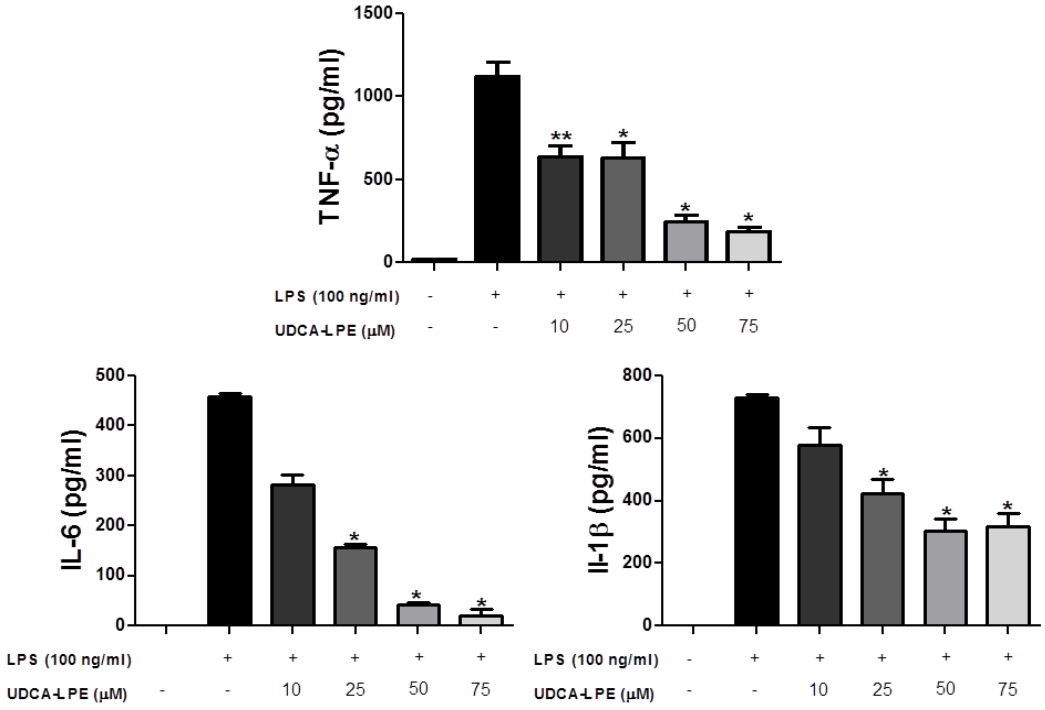

Figure 12:. Effect of UDCA-LPE on cytokine release in THP-1 differentiated macrophages. Cells were (or not) pre-treated with different concentration of UDCA-LPE in the range from 10 to 75 μM, followed by LPS (100 ng/ml) incubation for 24 hours. Results are presented as mean ± SD from three independent experiments, * $p<0.05$; **$p<0.01$ vs. LPS treatment alone.

7.2 Expression of COX-2 and iNOS

COX-2 and iNOS are inducible enzymes engaged in propagation of inflammatory response. Together they are rapid response genes because they do not require previous protein synthesis (Hwang 2001) and thus their manifestation in cells may be early detected. Their expression in LPS-treated THP-1 differentiated human macrophages was determined by Western blot analysis. For this purpose, cells were exposed to LPS (100 ng/ml) for 18 hours with or without previous pre-treatment with 50 or 75 μM UDCA-LPE. After treatment cells were harvested, the supernatant was collected, the amount of protein was normalized to 40 μg protein as described in Materials and Methods. Results are shown in the Figure 13. UDCA-LPE does not have a significant effect on iNOS neither COX-2 expression. However, these pro-inflammatory mediators were expressed already in control sample which suggests their activation likely by PMA used for the differentiation and moreover, the stimulation by LPS does not further increased their expression Because of this influence, I am not

able to assess the real effect of UDCA-LPE on COX-2 and iNOS within this experimental set up.

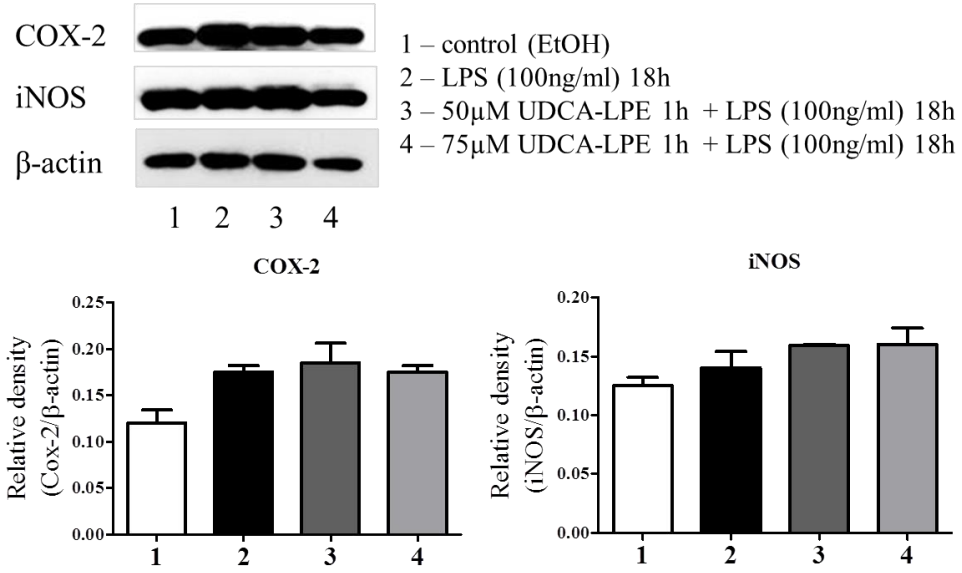

Figure 13: Effect of UDCA-LPE on COX-2 and iNOS expression. THP-1-derived macrophages were pre-treated with different concentration of UDCA-LPE as indicated in the pictures for 1 hour, then cells were stimulated by LPS (100 ng/ml) for 18 hours. The expression of COX-2 and iNOS was analyzed by Western blot. β-actin was used as internal control. Results are presented as mean ± SD from three independent experiments.

7.3 NFκB nuclear translocation

NFκB pathway is reported to be involved in LPS-induced inflammatory pathways via TLR4. Thus, its activation was determined by immunofluorescence, the whole procedures are described in Materials and Methods. First of all, the optimal time point for the maximal nuclear translocation of phosphorylated p65 (member of NFκB family) was fixed for 35 minutes (data not shown). With the aim to assess the effect of UDCA-LPE on p65 nuclear translocation of LPS-treated THP-1, differentiated macrophages were (or not) pre-treated with different concentrations of UDCA-LPE and subsequently incubated with LPS (100 ng/ml) for 35 minutes as established in the previous experiment. Conclusive pictures are shown in the Figure 14 and 16. To quantify the effect of UDCA-LPE on nuclear translocation of, phosphorylated p65, at least 300 cells from each coverslips were individually evaluated. UDC-LPE inhibits significantly, for about 50%, the translocation of phosphorylated p65 into the nucleus, see Figure 15.

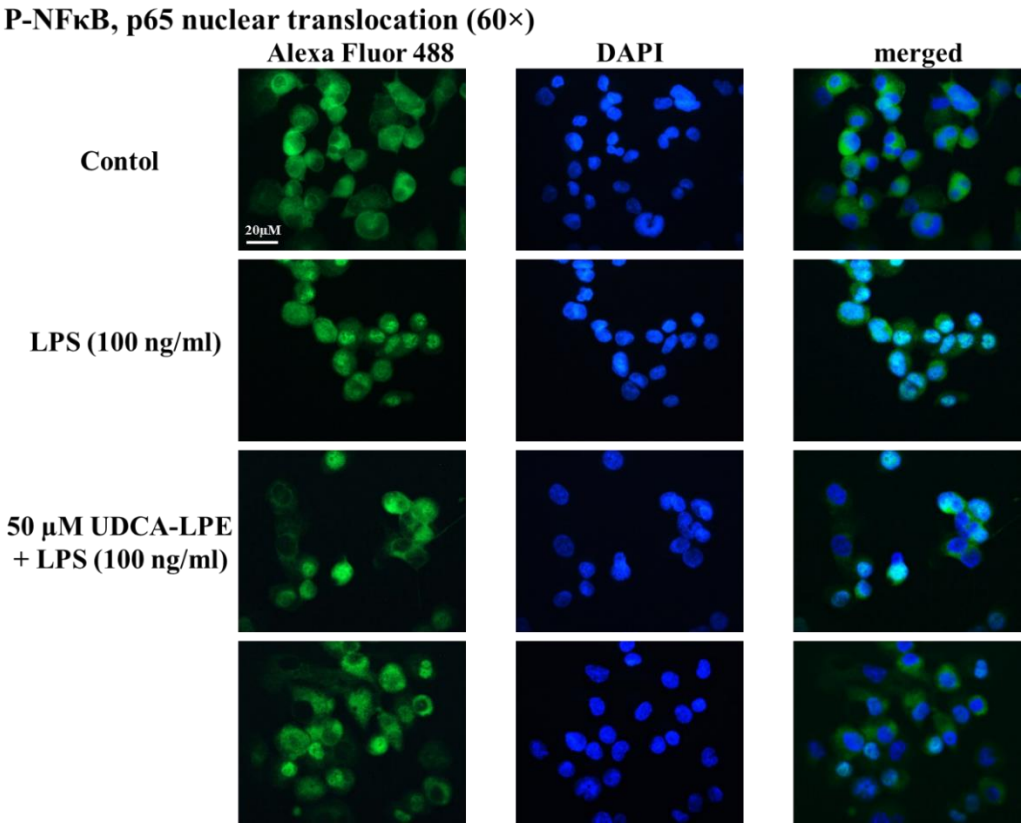

Figure 14: UDCA-LPE prevents nuclear translocation of NFκB in LPS treated differentiated THP-1, 60× magnification. Cells were pre-treated with above-mentioned concentrations of UDCA-LPE for 1 hour and subsequently stimulated by LPS (100 ng/ml) for 35 minutes, fixed in ice-cold methanol, stained with anti-phospho-p65 (NFκB) antibody visualized by secondary antibody Alexa Fluor 488 giving the green colour. Nuclei were stained with DAPI (in blue). When merged, the translocation of p65 into the nucleus gives rise to bright blue.

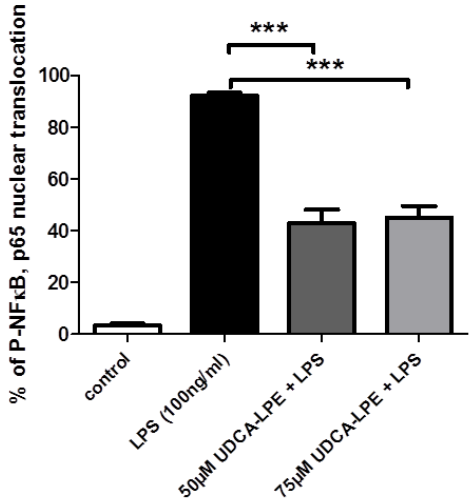

Figure 15: UDCA-LPE prevents nuclear translocation of NFκB, Results are presented as mean ± SD from six independent experiments, ***p<0.0001 vs. LPS treatment alone.

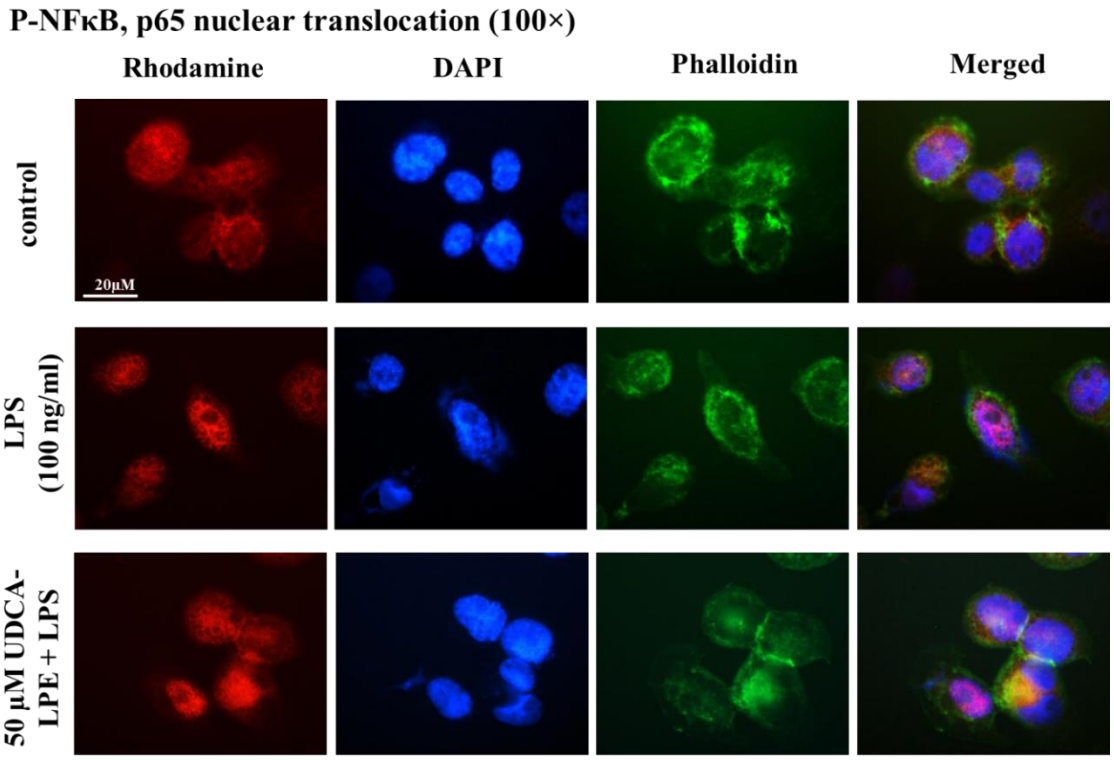

Figure 16: UDCA-LPE prevents nuclear translocation of NFκB in LPS treated differentiated THP-1, 100× magnification. Cells were pre-treated with mentioned concentration of UDCA-LPE for 1 hour and subsequently stimulated by LPS (100 ng/ml) for 35 minutes, fixed in ice-cold 4% formaldehyde, stained with anti-phospho-p65 (NFκB) antibody visualized by secondary antibody Rhodamin giving the red colour. Nuclei were stained with DAPI (in blue) and actin was labeled with Phalloidin CruzFluor (in green). When merger, nuclear translocation of p65 results in pink colour.

7.4 Activation of MAPK pathway - JNK upstream and downstream

To study whether and how UDCA-LPE possesses an inhibitory effect on the LPS-activated MAPK cascade further experiments were underwent. For this purpose, THP-1 differentiated macrophages were pre-treated with 50 or 75 µM UDCA-LPE for 1 hour and subsequently activated for 30 minutes with LPS (100 ng/ml). After treatment whole cell lysate were prepared and protein concentration was normalized to 25 µg/µl and samples were submitted to Western blot analysis. At first, the expression of three MAPK was determined.

LPS as well as UDCA-LPE do not have a significant influence on ERK expression (Figure 17) supporting the role of ERK as housekeeper protein, involved more in maintenance of cell process than in inflammatory response. On the other hand,

LPS caused an accentuated increase of all the other tested proteins involved in MAPK cascades. Moreover, UDCA-LPE significantly decreases the LPS-induced phosphorylation of p38, JNK1 and JNK2 in dose dependent manner. Whilst UDCA-LPE itself exhibits no effect on the phosphorylation of MAPK.

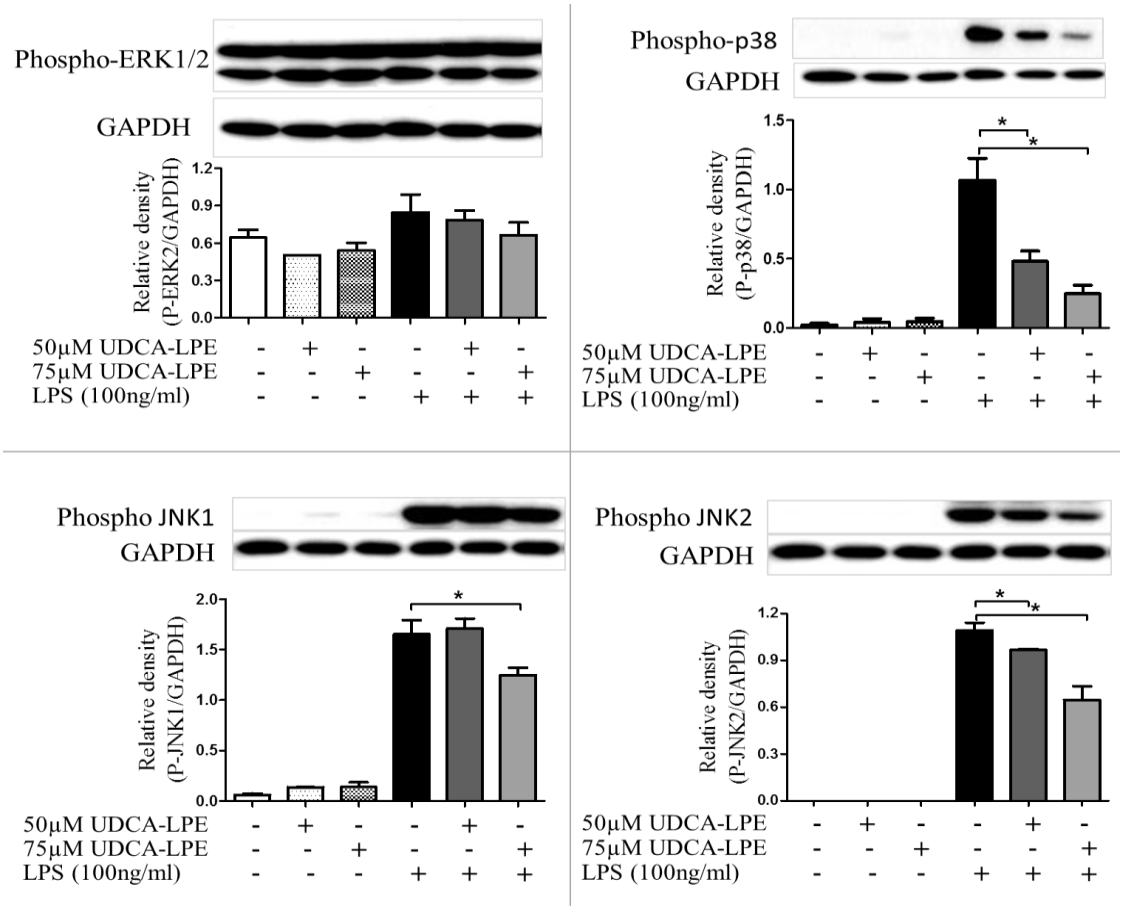

Figure 17: Effect of UDCA-LPE on LPS-induced signal transduction. THP-1-derived macrophages were pre-treated with different concentration of UDCA-LPE as indicated in the pictures for 1 hour, then cells were stimulated by LPS (100 ng/ml) for 30 minutes. The phosphorylation of ERK, p38 and JNK was analyzed by Western blot. GAPDH were used to verify the loading of samples. Results are presented as mean ± SD from three independent experiments, * $p<0.05$ vs. LPS treatment alone.

To further understand the mechanism by which UDCA-LPE inhibits JNK1/2 phosphorylation after LPS stimulation, their upstream activators were investigated. Both isoforms of JNK are activated by their MAPKK: MKK7 and MKK4. LPS induces the activation of both of these MAPKK and in turn their expression is significantly inhibited by UDCA-LPE in dose-dependent manner (Figure 18).

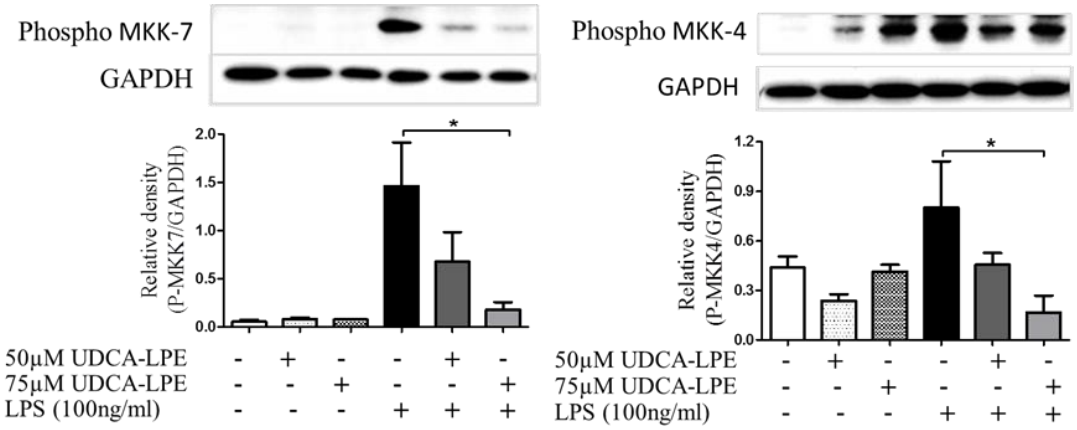

Figure 18: Effect of UDCA-LPE on LPS-induced JNK kinases – MKK7 and MKK4. THP-1-derived macrophages were pre-treated with different concentration of UDCA-LPE as indicated in the pictures for 1 hour, then cells were stimulated by LPS (100 ng/ml) for 30 minutes. The phosphorylation of MKKs was analyzed by Western blot. GAPDH were used to verify the loading of samples. Results are presented as mean ± SD from three independent experiments, * $p<0.05$ vs. LPS treatment alone.

Furthermore, the activation of downstream transcriptional factors, ATF-2 and c-Jun was determined by Western Blot and also by immunofluorescence. LPS activates their expression of both of these transcriptional factors in comparison to control. For ATF-2 expression, a slight tendency of the attenuation is observed while UDCA-LPE pre-treatment. Whereas, UDCA-LPE inhibits significantly the phosphorylation of c-Jun in dose-dependent manner (Figure 19).

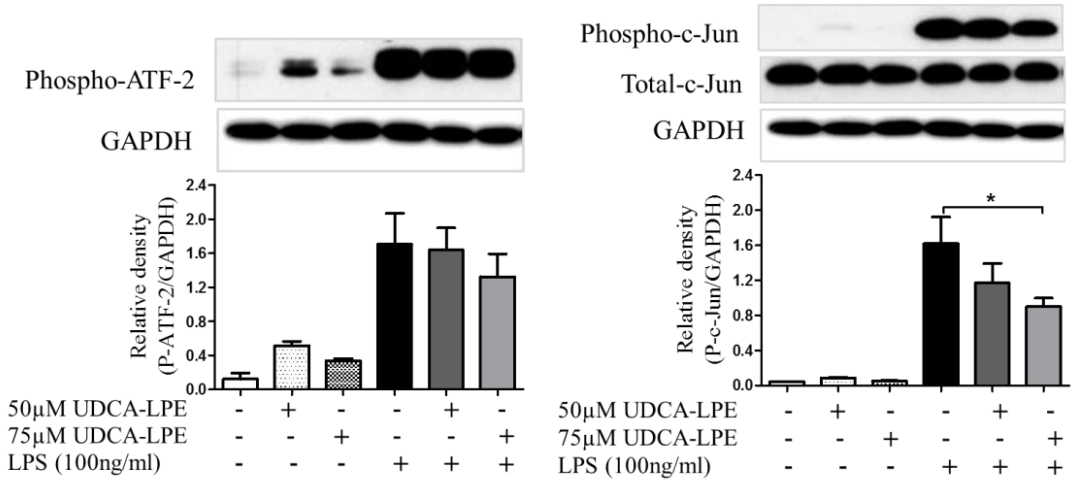

Figure 19: Effect of UDCA-LPE on LPS-induced phosphorylation of ATF-2 and c-Jun. THP-1-derived macrophages were pre-treated with different concentration of UDCA-LPE as indicated in the pictures for 1 hour, then cells were stimulated by LPS (100 ng/ml) for 30 minutes. The phosphorylation of transcriptional factors was analyzed by Western blot. GAPDH were used to verify the loading of samples. Results are presented as mean ± SD from three independent experiment, * $p<0.05$ vs. LPS treatment alone.

To visualize the nuclear translocation of above-mentioned transcriptional factors, cells after treatment were fixed in ice-cold methanol and investigated by immunofluorescence. UDCA-LPE partially disallows the condensation of ATF-2 and c-Jun in the nucleus (Figure 20 and 21). The results from both assays are consistent.

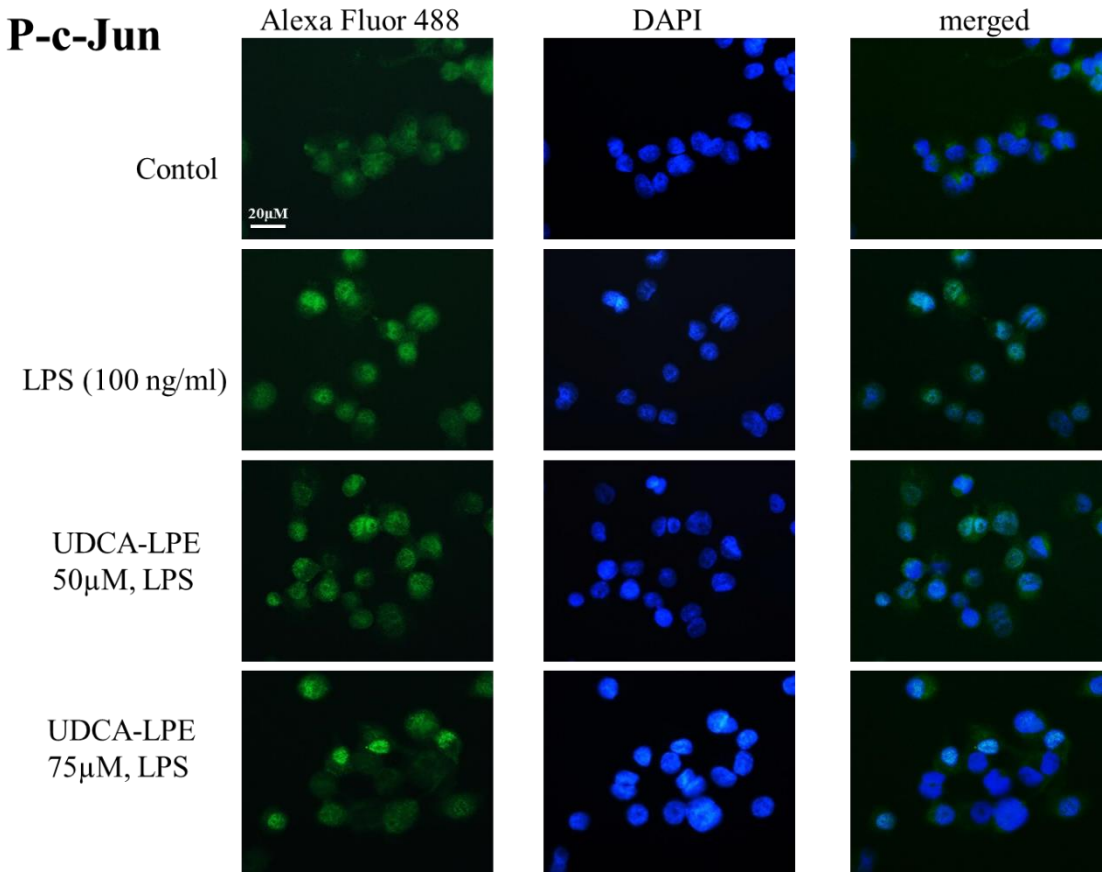

Figure 20: UDCA-LPE prevents nuclear translocation of c-Jun-2 transcriptional factor in LPS treated differentiated THP-1, 60× magnification. Cells were pre-treated with mentioned concentration of UDCA-LPE for 1 hour and subsequently stimulated by LPS (100 ng/ml) for 35 minutes, fixed in ice-cold methanol, stained with anti-phospho-c-Jun antibody visualized by secondary antibody Alexa Fluor 488 giving the green colour. Nuclei were stained with DAPI (in blue).

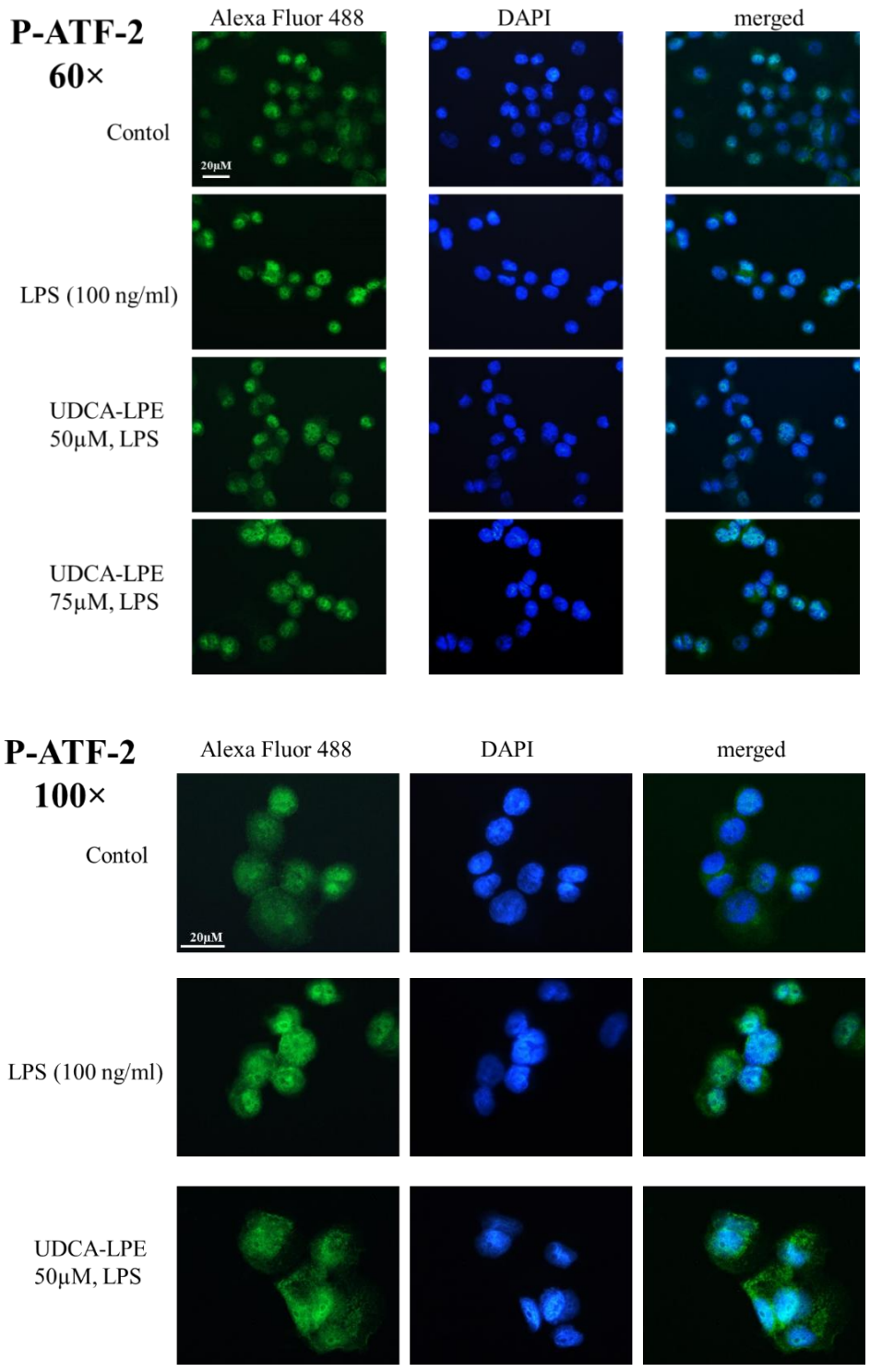

Figure 21: UDCA-LPE prevents nuclear translocation of ATF-2 transcriptional factor in LPS treated differentiated THP-1, 60× and 100× (B) magnification. Cells were pre-treated with mentioned concentration of UDCA-LPE for 1 hour and subsequently stimulated by LPS (100 ng/ml) for 35 minutes, fixed in ice-cold methanol, stained with anti-phospho-ATF-2 antibody visualized by secondary antibody Alexa Fluor 488 giving the green colour. Nuclei were stained with DAPI (in blue).

7.5 Recruitment of TRAF6 and Myd88 into the lipid rafts

While LPS stimulation TLR4 dimerizes and form the organized complex with accessory proteins MD-2 and CD14 in the lipid rafts. Recruitment of adaptor protein Myd88 and TRAF6 is necessary for engagement of MAPK signaling pathway as well as NFκB activation. To assess the ability of UDCA-LPE to interact with their recruitment into the lipid rafts, first, DRMs were isolated using Optiprep gradient and high speed ultracentrifugation as described in Materials and Methods, seven fractions were collected from the top to the bottom and analyzed by Western blot. Calnexin, protein enriched in endoplasmatic reticulum, were used as non-DRM marker, flotilin-2 as DRM marker. As shown in Figure 22, first 2 fractions can be considered as lipid raft fractions whereas fraction number 5-7 represent non-lipid raft, cytoplasmatic fractions.

Subsequently, presence of Myd88 and TRAF6 was determined. LPS as well as UDCA-LPE alone are able to recruit both of these adaptor proteins into the lipid rafts. However, there is no observed clear inhibition of recruitment of TRAF6 neither Myd88 when pre-treated with UDCA-LPE.

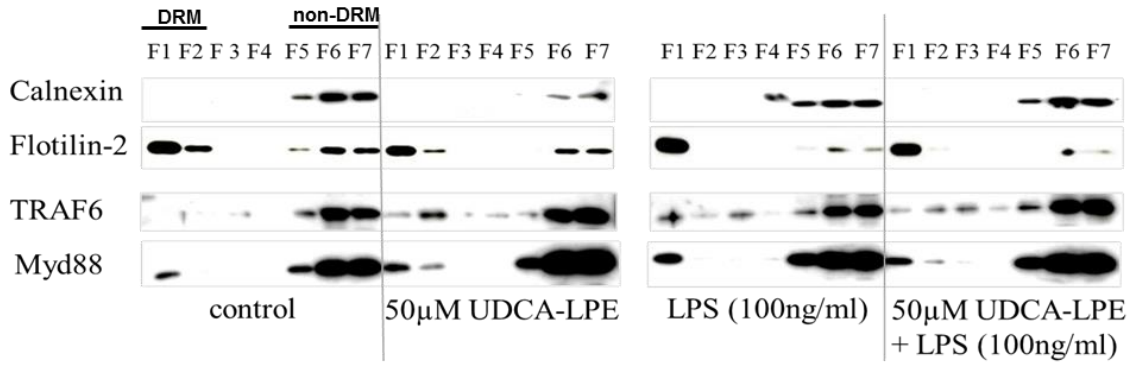

Figure 22: Recruitment of TRAF6 and MyD88 into the lipid rafts. Calnexin is used as non-DRM marker corresponding to non-lipid raft cellular fractions (F5 - F7) whereas flotilin-2 was used as DRM marker representing lipid raft fractions (F1-F2). Cells were pre-treated (or not) for 1 hour with 50 μM UDCA-LPE and subsequnetly treated with 100 ng/ml of LPS as marked in the figure.

8 DISCUSSION

UDCA-LPE is a new potential therapeutic agent in the therapy of fatty liver diseases – NASH, steatosis, NAFLD where the efficient treatment is still missing. Its hepatoprotective properties have been confirmed in several in vivo and in vitro studies. Moreover, UDCA-LPE possess anti-apoptotic, anti-inflammatory and also anti-fibrotic characteristics. How exactly UDCA-LPE fulfill this wide spectrum of properties is not fully understood yet. Its complex mechanism of action combines physico-chemical and biological activities.

The outcomes from MTT assay indicates that UDCA-LPE and the experimental set up are not cytotoxic and therefore are convenient for this study. Moreover, UDCA-LPE has shown to significantly increase metabolic activity of cells sustaining the capacity of UDCA-LPE for stimulation of growth and regeneration. These early results suggest UDCA-LPE as suitable for treatment when support of cell vitality and regeneration is needed. However, emanating from this predication, UDCA-LPE is unsuitable for a cancer treatment and a presence of any cancer should be excluded before the UDCA-LPE administration. This finding is in contrary with UDCA alone, which exhibits chemoprotective characteristics.

In this study, I have demonstrated that UDCA-LPE is able to significantly diminish LPS-initiated production of all tested pro-inflammatory cytokines (IL-6, IL-1β and TNFα) in a dose-dependent manner. Moreover, I have proved that UDCA-LPE enables to diminish nuclear translocation of NFκB about 50% at this may be one of the reasons for decreased cytokine production.

I have also proved that UDCA-LPE enables to inhibit the phosphorylation of two of three MAPK members – JNK1/2 and p38. It seems that UDCA-LPE has different effect on different JNK isoforms, its affects more strongly JNK2 than JNK1 isoform. The direct activators of JNKs are MKK4 together with MKK7. MKK7 distinctively phosphorylates JNK while MKK4 enables to activate p38 and MKK7 is principally responsible in phosphorylation of JNK whereas the concomitant phosphorylation by MKK4 regulates optimal JNK activity. In addition isoform-specific binding affinity of MKKs has been documented. MKK7 possesses higher affinity towards JNK2. (Haeusgen, Herdegen et al. 2010). These presumptions are in

accordance with my findings because MKK7 is more affected by UDCA-LPE while LPS and I can hypothesized then, that activation of JNKs is more important via MKK7 which is also more influenced by UDCA-LPE. LPS-activated JNKs via TLR4 are known to be inhibited by corticosteroids while such as dexamethasone that are nowadays one of the most important anti-inflammatory treatment (Swantek, Cobb et al. 1997). This supports the potential of UDCA-LPE as an anti-inflammatory drug.

A connecting element in regulation of both NFκB and MAPK signaling pathways is transforming growth factor β-activated kinase 1 (TAK1). TAK1 operates as a principal and positive mediator involved in inflammatory and immune signaling pathways in macrophages, fibroblasts as well as B cells. It functions as MAPKKK activating IKK complex as well as MKK4, 6 and 7 and therefore activating JNK and p38 in a cell-specific and receptor specific manner. (Chen, Hsu et al. 2015). Thus, the capacity of UDCA-LPE to inhibit engagement of TAK1 into the TLR4-associated complex or to modulate its phosphorylation may further clarify the mechanism of action of this bile acid-phospholipid conjugate.

In previous studies UDCA-LPE expressed capacity to modulate composition of fatty acid pool from cytotoxic saturated towards protective polyunsaturated fatty acids (PUFAs) and therefore restraining apoptosis (Chamulitrat, Liebisch et al. 2013). In addition, it has been documented that PUFAs, especially ω-3 PUFAs represented typically by eicosapentaenoic and docosahexanoic acids, possesses anti-inflammatory properties through modulation of cell metabolism, gene expression and production of pro-inflammatory mediators in multiple levels (Nakakuki, Kawano et al. 2013, Sekhon-Loodu, Ziaullah et al. 2015). Moreover, fatty acids have shown to reciprocally regulate activation of inflammatory signaling pathways via modulation of dimerization of TLR4 and its recruitment into the lipid rafts. Saturated fatty acids support its recruitment and association with further adaptor proteins (MD-2, MyD88, TRIF, TRAF6) in order to initiate downstream signaling whereas PUFAs inhibit formation of this complex (Wong, Kwon et al. 2009).

Additionally, UDCA-LPE exhibits similar properties with liver X receptors (LXRs) which regulates metabolism of lipids and cholesterol in transcriptional level and anti-inflammatory capacity via suppression of TLR-mediated MAPK and NFκB signaling cascades . Their ability to suppress association of adaptor protein MyD88 and

TRAF6 into the lipid rafts and therefore triggering the downstream pathways has been discovered (Ito, Hong et al. 2015). Natural LXRs agonists are oxysterols which as well as UDCA-LPE possess steroid structure (Loren, Huang et al. 2013).

These findings have motivated me to investigate if and how is UDCA-LPE able to influence recruitment of adaptor proteins Myd88 and TRAF6 into the lipid rafts. The isolation of lipid rafts has shown that LPS stimulation initiates the translocation of adaptor protein MyD88 and TRAF6 into the lipid rafts but when pretreated with UDCA-LPE, the recruitment of afore-mentioned proteins seem to be partially suppressed. Surprisingly, UDCA-LPE alone has shown to initiate activation of investigated proteins into the lipid rafts. Deeper investigations with different time set up could provide more details what is happening in the membrane while UDCA-LPE treatment. And also, the assessment of UDCA-LPE as possible LXR agonist would be helpful in clarifying the mechanism of versatility of this hepaprotectant compound.

Anti-inflammatory mechanism of action of UDCA-LPE is summarized on Figure 23.

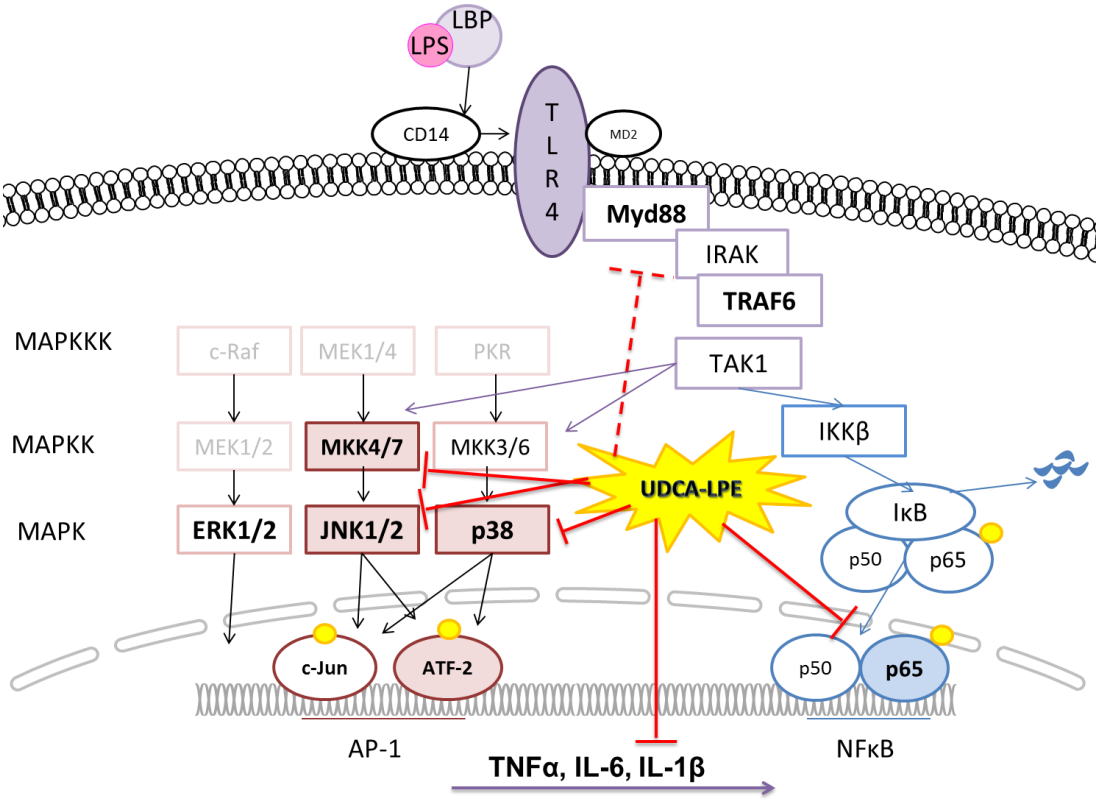

Figure 23: Schema summarizing the targets of anti-inflammatory mechanism of action of UDCA-LPE in LPS-induced THP-1 derived human macrophages.

9 CONCLUSION

In this study I have demonstrated that UDCA-LPE suppresses LPS-induced production of potent inflammatory cytokines (TNFα, IL-6 and IL-1β) in human THP-1-derived macrophages. Its mechanism of action of anti-inflammatory properties is complex. UDCA-LPE enables to quench phosphorylation of both JNK isoforms and p38 and additionally, it has ability to inhibit NFκB nuclear translocation.

Thus I may estimate that UDCA-LPE could exhibit its hepatoprotective properties also via modulation of immune system. Due to its versatility, UDCA-LPE has a potential to become a novel therapeutic approach for treatment of NASH.

10 REFERENCES

Blasius, A. L. and B. Beutler (2010). "Intracellular toll-like receptors." Immunity **32**(3): 305-315.

Blazovics, A., et al. (2004). "[Cytokines, prostaglandins, nutritive and non-nuitritive factors in inflammatory bowel diseases]." Orv Hetil **145**(50): 2523-2529.

Broz, P. and D. M. Monack (2013). "Newly described pattern recognition receptors team up against intracellular pathogens." Nat Rev Immunol **13**(8): 551-565.

Brubaker, S. W., et al. (2015). "Innate immune pattern recognition: a cell biological perspective." Annu Rev Immunol **33**: 257-290.

Centuori, S. M. and J. D. Martinez (2014). "Differential regulation of EGFR-MAPK signaling by deoxycholic acid (DCA) and ursodeoxycholic acid (UDCA) in colon cancer." Dig Dis Sci **59**(10): 2367-2380.

De Nardo, D. (2015). "Toll-like receptors: Activation, signalling and transcriptional modulation." Cytokine **74**(2): 181-189.

Dobrovolskaia, M. A. and S. N. Vogel (2002). "Toll receptors, CD14, and macrophage activation and deactivation by LPS." Microbes Infect **4**(9): 903-914.

Donaldson, J. G. (2015). "Immunofluorescence Staining." Curr Protoc Cell Biol **69**: 4 3 1-7.

Fiorucci, S., et al. (2001). "NCX-1000, a NO-releasing derivative of ursodeoxycholic acid, selectively delivers NO to the liver and protects against development of portal hypertension." Proc Natl Acad Sci U S A **98**(15): 8897-8902.

Guarino, M. P., et al. (2013). "Ursodeoxycholic acid therapy in gallbladder disease, a story not yet completed." World J Gastroenterol **19**(31): 5029-5034.

Guha, M. and N. Mackman (2001). "LPS induction of gene expression in human monocytes." Cell Signal **13**(2): 85-94.

Haeusgen, W., et al. (2010). "Specific regulation of JNK signalling by the novel rat MKK7gamma1 isoform." Cell Signal **22**(11): 1761-1772.

Hayden, M. S. and S. Ghosh (2008). "Shared principles in NF-kappaB signaling." Cell **132**(3): 344-362.

Huang, S., et al. (2012). "Saturated fatty acids activate TLR-mediated proinflammatory signaling pathways." J Lipid Res **53**(9): 2002-2013.

Hwang, D. (2001). "Modulation of the expression of cyclooxygenase-2 by fatty acids mediated through toll-like receptor 4-derived signaling pathways." Faseb j **15**(14): 2556-2564.

Chamulitrat, W., et al. (2009). "Bile salt-phospholipid conjugate ursodeoxycholyl lysophosphatidylethanolamide as a hepatoprotective agent." Hepatology **50**(1): 143-154.

Chamulitrat, W., et al. (2013). "Ursodeoxycholyl lysophosphatidylethanolamide inhibits lipoapoptosis by shifting fatty acid pools toward monosaturated and polyunsaturated fatty acids in mouse hepatocytes." Mol Pharmacol **84**(5): 696-709.

Chen, I. T., et al. (2015). "Polyubiquitination of Transforming Growth Factor beta-activated Kinase 1 (TAK1) at Lysine 562 Residue Regulates TLR4-mediated JNK and p38 MAPK Activation." Sci Rep **5**: 12300.

Ito, A., et al. (2015). "LXRs link metabolism to inflammation through Abca1-dependent regulation of membrane composition and TLR signaling." Elife **4**: e08009.

Jimenez-Dalmaroni, M. J., et al. (2016). "The critical role of toll-like receptors - From microbial recognition to autoimmunity: A comprehensive review." Autoimmun Rev **15**(1): 1-8.

Johnson, G. L. and K. Nakamura (2007). "The c-jun kinase/stress-activated pathway: regulation, function and role in human disease." Biochim Biophys Acta **1773**(8): 1341-1348.

Jones, H., et al. (2015). "Bile acid signaling and biliary functions." Acta Pharm Sin B **5**(2): 123-128.

Kaminska, B. (2005). "MAPK signalling pathways as molecular targets for anti-inflammatory therapy--from molecular mechanisms to therapeutic benefits." Biochim Biophys Acta **1754**(1-2): 253-262.

Kim, E. K. and E. J. Choi (2015). "Compromised MAPK signaling in human diseases: an update." Arch Toxicol **89**(6): 867-882.

Kim, J. A., et al. (2011). "Anti-inflammatory action of sulfated glucosamine on cytokine regulation in LPS-activated PMA-differentiated THP-1 macrophages." Inflamm Res **60**(12): 1131-1138.

Kleinert, H., et al. (2003). "Regulation of the expression of inducible nitric oxide synthase." Biol Chem **384**(10-11): 1343-1364.

Korbecki, J., et al. (2013). "The effect of reactive oxygen species on the synthesis of prostanoids from arachidonic acid." J Physiol Pharmacol **64**(4): 409-421.

Kotb, M. A. (2012). "Molecular mechanisms of ursodeoxycholic acid toxicity & side effects: ursodeoxycholic acid freezes regeneration & induces hibernation mode." Int J Mol Sci **13**(7): 8882-8914.

Li, Z., et al. (2006). "The ratio of phosphatidylcholine to phosphatidylethanolamine influences membrane integrity and steatohepatitis." Cell Metab **3**(5): 321-331.

Lin, W. J. and W. C. Yeh (2005). "Implication of Toll-like receptor and tumor necrosis factor alpha signaling in septic shock." Shock **24**(3): 206-209.

Lingwood, D. and K. Simons (2007). "Detergent resistance as a tool in membrane research." Nat Protoc **2**(9): 2159-2165.

Loren, J., et al. (2013). "Liver X receptor modulators: a review of recently patented compounds (2009 - 2012)." Expert Opin Ther Pat **23**(10): 1317-1335.

Lowry, O. H., et al. (1951). "Protein measurement with the Folin phenol reagent." J Biol Chem **193**(1): 265-275.

Luo, J. L., et al. (2005). "IKK/NF-kappaB signaling: balancing life and death--a new approach to cancer therapy." J Clin Invest **115**(10): 2625-2632.

Mandrekar, P. and G. Szabo (2009). "Signalling pathways in alcohol-induced liver inflammation." J Hepatol **50**(6): 1258-1266.

Mosmann, T. (1983). "Rapid colorimetric assay for cellular growth and survival: application to proliferation and cytotoxicity assays." J Immunol Methods **65**(1-2): 55-63.

Nakakuki, M., et al. (2013). "Eicosapentaenoic acid suppresses palmitate-induced cytokine production by modulating long-chain acyl-CoA synthetase 1 expression in human THP-1 macrophages." Atherosclerosis **227**(2): 289-296.

Opal, S. M., et al. (1999). "Relationship between plasma levels of lipopolysaccharide (LPS) and LPS-binding protein in patients with severe sepsis and septic shock." J Infect Dis **180**(5): 1584-1589.

Pathil, A., et al. (2014). "Ursodeoxycholyl lysophosphatidylethanolamide attenuates hepatofibrogenesis by impairment of TGF-beta1/Smad2/3 signalling." Br J Pharmacol **171**(22): 5113-5126.

Pathil, A., et al. (2012). "Ursodeoxycholyl lysophosphatidylethanolamide improves steatosis and inflammation in murine models of nonalcoholic fatty liver disease." Hepatology **55**(5): 1369-1378.

Pathil, A., et al. (2011). "The synthetic bile acid-phospholipid conjugate ursodeoxycholyl lysophosphatidylethanolamide suppresses TNFalpha-induced liver injury." J Hepatol **54**(4): 674-684.

Pathil, A., et al. (2012). "Comparison of different bile acid-phospholipid conjugates in acute hepatitis." Eur J Clin Invest **42**(2): 130-138.

Peterson, G. L. (1979). "Review of the Folin phenol protein quantitation method of Lowry, Rosebrough, Farr and Randall." Anal Biochem **100**(2): 201-220.

Pike, L. J. (2003). "Lipid rafts: bringing order to chaos." J Lipid Res **44**(4): 655-667.

Poupon, R. (2012). "Ursodeoxycholic acid and bile-acid mimetics as therapeutic agents for cholestatic liver diseases: an overview of their mechanisms of action." Clin Res Hepatol Gastroenterol **36 Suppl 1**: S3-12.

Reuven, E. M., et al. (2014). "Regulation of innate immune responses by transmembrane interactions: lessons from the TLR family." Biochim Biophys Acta **1838**(6): 1586-1593.

Roda, A., et al. (1990). "Bile acid structure-activity relationship: evaluation of bile acid lipophilicity using 1-octanol/water partition coefficient and reverse phase HPLC." J Lipid Res **31**(8): 1433-1443.

Roma, M.G. et al. (2011). "Ursodeoxycholic acid in cholestasis: linking action mechanisms to therapeutic applications." Clinical Science **121**(12): 523-544.

Ruysschaert, J. M. and C. Lonez (2015). "Role of lipid microdomains in TLR-mediated signalling." Biochim Biophys Acta **1848**(9): 1860-1867.

Sabio, G. and R. J. Davis (2014). "TNF and MAP kinase signalling pathways." Semin Immunol **26**(3): 237-245.

Sekhon-Loodu, S., et al. (2015). "Docosahexaenoic acid ester of phloridzin inhibit lipopolysaccharide-induced inflammation in THP-1 differentiated macrophages." Int Immunopharmacol **25**(1): 199-206.

Simons, K. and R. Ehehalt (2002). "Cholesterol, lipid rafts, and disease." J Clin Invest **110**(5): 597-603.

Simons, K. and J. L. Sampaio (2011). "Membrane organization and lipid rafts." Cold Spring Harb Perspect Biol **3**(10): a004697.

Stokes, C. S., et al. (2014). "Ursodeoxycholic acid and diets higher in fat prevent gallbladder stones during weight loss: a meta-analysis of randomized controlled trials." Clin Gastroenterol Hepatol **12**(7): 1090-1100.e1092; quiz e1061.

Swantek, J. L., et al. (1997). "Jun N-terminal kinase/stress-activated protein kinase (JNK/SAPK) is required for lipopolysaccharide stimulation of tumor necrosis factor alpha (TNF-alpha) translation: glucocorticoids inhibit TNF-alpha translation by blocking JNK/SAPK." Mol Cell Biol **17**(11): 6274-6282.

Vang, S., et al. (2014). "The Unexpected Uses of Urso- and Tauroursodeoxycholic Acid in the Treatment of Non-liver Diseases." Glob Adv Health Med **3**(3): 58-69.

Wasserman, S. A. (2000). "Toll signaling: the enigma variations." Curr Opin Genet Dev **10**(5): 497-502.

Wong, S. W., et al. (2009). "Fatty acids modulate Toll-like receptor 4 activation through regulation of receptor dimerization and recruitment into lipid rafts in a reactive oxygen species-dependent manner." J Biol Chem **284**(40): 27384-27392.

Xiang, Z., et al. (2013). "The role of ursodeoxycholic acid in non-alcoholic steatohepatitis: a systematic review." BMC Gastroenterol **13**: 140.

Yoshino, H., et al. (2014). "Ionizing radiation affects the expression of Toll-like receptors 2 and 4 in human monocytic cells through c-Jun N-terminal kinase activation." J Radiat Res **55**(5): 876-884.

Zhu, G. Q., et al. (2015). "A network meta-analysis of the efficacy and side effects of udca-based therapies for primary sclerosing cholangitis." Oncotarget **6**(29): 26757-26769.

Zhu, G. Q., et al. (2015). "Network meta-analysis of randomized controlled trials: efficacy and safety of UDCA-based therapies in primary biliary cirrhosis." Medicine (Baltimore) **94**(11): e609.